2022-12

ANALYSIS OF IDEAL MANEUVERS FOR MISSION EXTENSION VEHICLE

Mathies, Max S.

Monterey, CA; Naval Postgraduate School

NAVAL POSTGRADUATE SCHOOL

MONTEREY, CALIFORNIA

THESIS

ANALYSIS OF IDEAL MANEUVERS FOR MISSION EXTENSION VEHICLE

by

Max S. Mathies

December 2022

Thesis Advisor: Marcello Romano
Co-Advisor: Jennifer Hudson

THIS PAGE INTENTIONALLY LEFT BLANK

REPORT DOCUMENTATION PAGE	*Form Approved OMB No. 0704-0188*

1. AGENCY USE ONLY *(Leave blank)*	**2. REPORT DATE** December 2022	**3. REPORT TYPE AND DATES COVERED** Master's thesis

4. TITLE AND SUBTITLE
ANALYSIS OF IDEAL MANEUVERS
FOR MISSION EXTENSION VEHICLE

5. FUNDING NUMBERS

6. AUTHOR(S) Max S. Mathies

7. PERFORMING ORGANIZATION NAME(S) AND ADDRESS(ES)
Naval Postgraduate School
Monterey, CA 93943-5000

8. PERFORMING ORGANIZATION REPORT NUMBER

9. SPONSORING / MONITORING AGENCY NAME(S) AND ADDRESS(ES)
N/A

10. SPONSORING / MONITORING AGENCY REPORT NUMBER

11. SUPPLEMENTARY NOTES The views expressed in this thesis are those of the author and do not reflect the official policy or position of the Department of Defense or the U.S. Government.

12a. DISTRIBUTION / AVAILABILITY STATEMENT
Approved for public release. Distribution is unlimited.

12b. DISTRIBUTION CODE
A

13. ABSTRACT (maximum 200 words)

Finding optimal maneuvers between spacecraft is computationally demanding. Targeting many spacecraft successively requires more computational power than commercially available. This thesis tested algorithms looking to reduce this computational burden. Algorithms claiming optimal two-impulse rendezvous solutions between any two arbitrary orbits were coded and compared through minimum delta-vs (fuel) and computational times. Orbit characteristics were varied across a multitude of scenarios to represent many possible applications. Assorted considerations were discussed, which provided a framework for designing multi-client on-orbit servicing missions.

14. SUBJECT TERMS
orbital mechanics, GPOPS, proximity maneuvers, space flight, keplerian two body problem, circular orbit, mission extension vehicle, orbiting spacecraft, geosynchronous orbit, circular orbit, restricted kepler problem, Hill-Clohessy-Wiltshire, HCW, chief, deputy, linearized equations, optimization, traveling salesman, vehicle routing, TSP

15. NUMBER OF PAGES
89

16. PRICE CODE

17. SECURITY CLASSIFICATION OF REPORT	**18. SECURITY CLASSIFICATION OF THIS PAGE**	**19. SECURITY CLASSIFICATION OF ABSTRACT**	**20. LIMITATION OF ABSTRACT**
Unclassified	Unclassified	Unclassified	UU

NSN 7540-01-280-5500

Standard Form 298 (Rev. 2-89)
Prescribed by ANSI Std. 239-18

THIS PAGE INTENTIONALLY LEFT BLANK

Approved for public release. Distribution is unlimited.

ANALYSIS OF IDEAL MANEUVERS FOR MISSION EXTENSION VEHICLE

Max S. Mathies
Lieutenant, United States Navy
BA, Duke University, 2010

Submitted in partial fulfillment of the
requirements for the degree of

MASTER OF SCIENCE IN ASTRONAUTICAL ENGINEERING

from the

NAVAL POSTGRADUATE SCHOOL
December 2022

Approved by: Marcello Romano
Advisor

Jennifer Hudson
Co-Advisor

Brian S. Bingham
Chair, Department of Mechanical and Aerospace Engineering

THIS PAGE INTENTIONALLY LEFT BLANK

ABSTRACT

Finding optimal maneuvers between spacecraft is computationally demanding. Targeting many spacecraft successively requires more computational power than commercially available. This thesis tested algorithms looking to reduce this computational burden. Algorithms claiming optimal two-impulse rendezvous solutions between any two arbitrary orbits were coded and compared through minimum delta-vs (fuel) and computational times. Orbit characteristics were varied across a multitude of scenarios to represent many possible applications. Assorted considerations were discussed, which provided a framework for designing multi-client on-orbit servicing missions.

THIS PAGE INTENTIONALLY LEFT BLANK

Table of Contents

List of Figures

List of Tables

THIS PAGE INTENTIONALLY LEFT BLANK

List of Acronyms and Abbreviations

C2C	Circular to Circular
C2E	Circular to Elliptical
COE	Classical Orbital Elements
DARPA	Defense Advanced Research Projects Agency
DIU	Defense Innovation Unit
DOD	Department of Defense
E2C	Elliptical to Circular
E2E	Elliptical to Elliptical
GEO	Geosynchronous Earth Orbit
HEO	Highly Elliptical Orbit
K2BP	Kepler Two-Body Problem
kg	kilograms
km	Kilometers
LEO	Low Earth Orbit
MBSE	Model-Based System Engineering
MEO	Medium Earth Orbit
MEV	Mission Extension Vehicle
mo	Months
NASA	National Aeronautics and Space Administration

OOS	On-Orbit Servicing
s	Seconds
SWaP	Size, Weight, and Power
TSP	Traveling Salesman Problem
VRP	Vehicle Routing Problem

Acknowledgments

Thank you to all the members of my graduating class. We would not have gotten very far without each other.

Thank you to all the SRL team for listening to hours of brainstorming and for the help in focusing the results to clear ideas.

Thank you Dr. Marcello Romano and Dr. Jennifer Hudson for allowing me to ride your intellectual coattails. You gave me your time and I soaked up as much as I could. I am forever in your debt for allowing me to achieve my only goal coming to NPS, which was to push myself academically.

Thank you to my family for supporting Noelle and me on this journey.

Thank you Noelle, the love of my life, for everything.

THIS PAGE INTENTIONALLY LEFT BLANK

CHAPTER 1:
Introduction

1.1 Background

As of January 1st, 2022, there are 4,852 satellites orbiting Earth. Of these, 4,078 are in Low Earth Orbit (LEO), 141 are in Medium Earth Orbit (MEO), 59 are in Highly Elliptical Orbit (HEO), and 574 are in Geosynchronous Earth Orbit (GEO) [1]. The growth in space leads to a similar trend in the concern over space logistics. In 2022, SpaceX advertised the use of a reusable launch vehicle, the Falcon Heavy, for $97M capable of carrying 68,000 kilograms (kg) to LEO [2], equating to $1425/kg. Even with the reducing costs required to send material to orbit, there is an apparent market to service existing spacecraft, instead of sending an entire replacement spacecraft [3], [4].

There is a current need to service exquisite space systems to extend their life. This is mostly due to a depletion of fuel from operating beyond the intended end of life for the mission or from failures in replaceable or repairable components or subsystems [5]. An On-Orbit Servicing (OOS) satellite can carry fuel, parts, tools, and a robotic arm to manipulate or deliver all of these. The Mission Extension Vehicle (MEV) produced by Northrop Grumman [6] represents recent commercial development in this area, including the launches of MEV-1 and MEV-2 in 2019 and 2020, respectively. Prior to missions like these, servicing operations were performed by humans such as the ones for the Hubble Space Telescope [4]. It wasn't until 2007, when the Defense Advanced Research Projects Agency (DARPA) and National Aeronautics and Space Administration (NASA) launched Orbital Express, which was the first US mission to transfer components between spacecraft, unassisted [7]. The result is a peaking interest in cost analysis, with the hope of savings from servicing satellites that have fallen into disrepair or increasing flexibility in mission design with unlimited potential for modular replacements. If OOS spacecraft were mainstreamed, any space mission could reduce up front costs and save Size, Weight, and Power (SWaP) due to less fuel or survivability required in design.

In addition to serviceable spacecraft, orbital debris has increased drastically with over 25,000

trackable pieces over 10 cm in diameter in LEO alone [8]. Even though the atmosphere produces enough drag at high enough altitudes to slow most of these pieces causing them to accelerate back to Earth, models suggest that there are enough traffic and collisions to produce more debris than atmospheric drag would remove from orbit, with potential for exponential increase if no debris protection or mitigation measures are put in place and followed [8]. This provides another market for OOS satellites doing debris remediation through active debris removal.

Astrodynamics is the application of mechanics to problems derived from considering the motion of masses in space. When considering multiple spacecraft in orbit around Earth, it is practically relevant to consider travel between them. Intuitively, most would assume a straight line to be the best way to do that. However, applying force to a spacecraft where the only other force acting on it is the force of gravity from Earth is difficult to conceive naturally, given how different the frame of reference is from our daily experience. Consider the scenario in Figures 1.1 through 1.3, where there are two spacecraft in the same circular orbit around Earth.

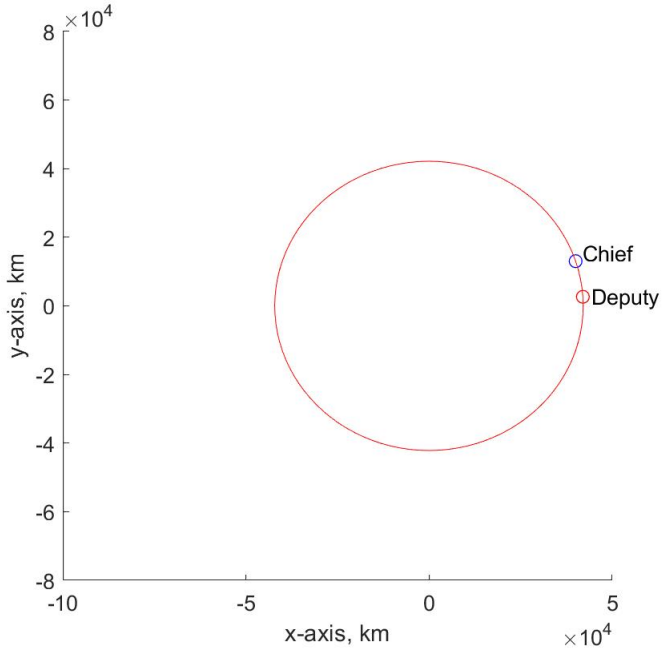

Figure 1.1. Initial Orientation of Chief and Deputy

A deputy spacecraft prepares to move to the chief.

A deputy is a chaser spacecraft to which we apply another force besides gravity. What happens if we try applying force to the deputy in the direction of the chief as most intuition suggests? See Figure 1.2.

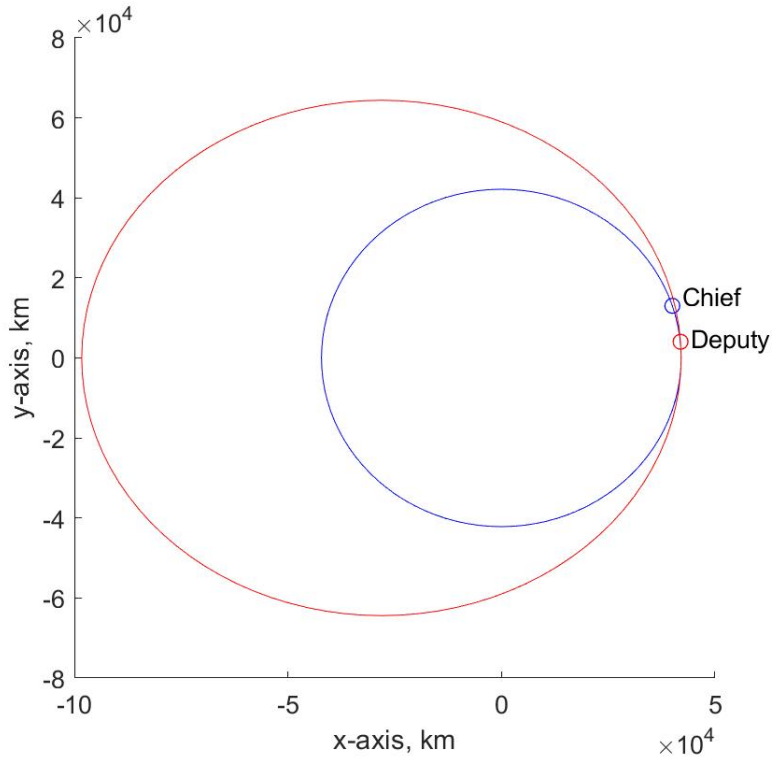

Figure 1.2. Second Orientation of Chief and Deputy

After force applied to deputy, its orbit changes.

Since the force applied was in the direction of the velocity, there is energy added to the deputy's orbit, allowing it to travel further from Earth. At the end of the instantaneous addition of energy, in other words an impulsive burn, the deputy is in an elliptical orbit instead of the circular and is at the orbit's periapsis, or closest point to Earth. If we step forward in time with no additional changes we can watch what happens in Figure 1.3.

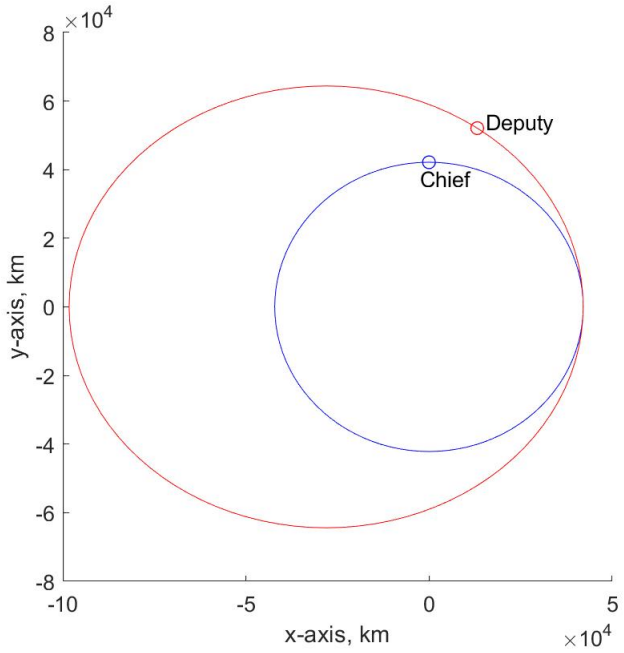

Figure 1.3. Third Orientation of Chief and Deputy

With the new orbit, the distance increases between them, instead of the intuitive decrease.

This simple demonstration illustrates the confusion the first pilots in space must have felt when they realized applying thrust toward your target would take you further from it and they essentially needed to apply the brakes, or thrust away from their target, in order to accelerate towards it. In other words, slow down to speed up and speed up to slow down. This phasing maneuver and other well understood orbital transfer problems, such as Hohmann and coplanar elliptical, will be further explained in Chapter 3.

Much of the literature explaining mission design for OOS spacecraft has shown limitations due to focus on simple astrodynamic scenarios or assumption of accurate algorithms. This thesis aimed to identify non-intuitive orbital maneuvers and produced new algorithms to compare with existing ones for locating possible inefficiencies in current operations and filling the gap for OOS mission design for many clients by comparing increasingly complex scenarios and computation power required for accurate algorithms.

1.2 Problem

Optimal two-impulse burn rendezvous maneuvers between two orbital states were explored using various parameters and techniques. When trying to find a brute force absolute optimal route between all possible states (or nodes) on two arbitrary orbits, the computational power was too burdensome to implement without a supercomputer, and would be impossible on board a spacecraft. In planning a servicing mission for a satellite, optimal or near-optimal routes can increase the number of satellites serviced or decrease the cost of such missions. For several cases of orbital transfer problems, local quasi-optimal solutions were computed by various algorithms and compared. A guide to planning an optimal route between possible nodes was developed with traveling salesman and vehicle routing problems in mind. This guide could fill a gap in current inefficient operational planning and computational power allocation.

1.3 Objective

This thesis aimed to produce and compare results from applying algorithms to solving computationally demanding sets of serial orbital maneuver problems against optimal or quasi-optimal solutions.

1.4 Model-Based Systems Engineering

Development and presentation of this thesis was assisted by the use of Model-Based System Engineering (MBSE), a formal approach for the use of models as the primary tool for information exchange. It helped narrowed the scope and highlight the gap in current applications this thesis attempted to fill.

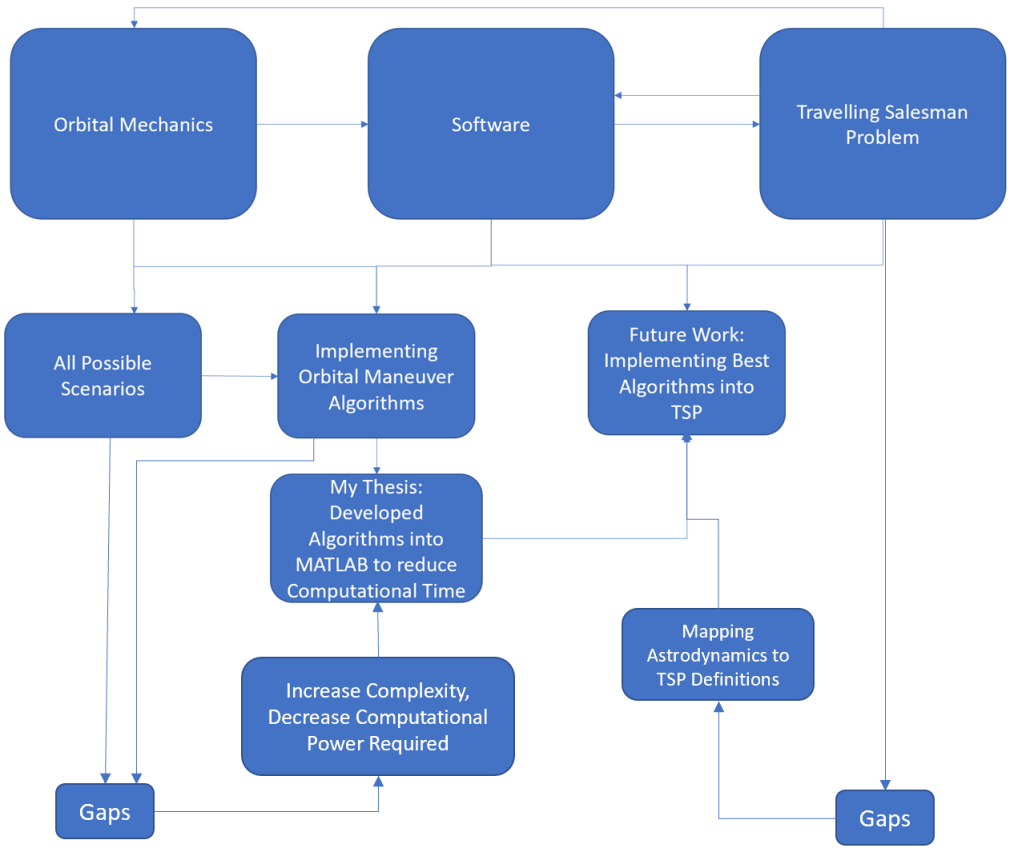

Figure 1.4. MBSE Model 2

This type of information organization proved useful throughout the thesis.

1.5 Current Practices

The two resources that are considered most valuable in space are time and mass. With more of either of these, any problem can be solved. Researchers around the world are figuring out how to send more to space, faster, with better lifespans. One of the intersections of this research is how to reduce the amount of fuel needed to move a spacecraft from one orbit to many successive orbits. The evaluated research shows a reliance on using solutions to Lambert's problem, varying parameters, and comparing the change in velocities (fuel) required for

large lists of individual solutions [9], [10], [11]. A solution that considers all possible trajectories, also known as the brute force method, is too computationally demanding for supercomputers to determine the best route for many clients. Attempts at reducing the list size have been relatively successful using Traveling Salesman Problem (TSP) algorithms, further discussed in Chapter 4.3 [9], [10], [11].

1.6 Methodology

This thesis simulated increasingly complex relative orbit relationships and generated solutions and computation times for optimal or quasi-optimal solutions through various algorithms in MATLAB software, most of which was sourced, some was adapted.

Chapter 2 provides the basis for all closed-form solutions to orbital maneuvers including a summary of assumptions, an establishment of common vernacular for orbital elements, an introduction to the earth-centered inertial reference frame, and a proof from familiar laws in physics to a widely used relationship between position and acceleration.

Chapter 3 contains a baseline of commonly used maneuvers and an introduction to the algorithms used for comparison.

Chapter 4 lists two considerations for an end user with the intention to help build a framework for decision-making based on types of orbits that need planned visits.

Chapter 5 lists the results comparing algorithms with delta-vs and computational times.

Chapter 6 highlights potential singularities and trends as a conclusion and identifies future work and how this can be implemented into TSP algorithms to reduce current computational estimates at different levels based on desired integrity of the results.

THIS PAGE INTENTIONALLY LEFT BLANK

CHAPTER 2:
Problem Setup

2.1 Restricted Keplerian Two-Body Problem

In order to work on practical problems related to motion of a spacecraft around Earth, observed were a set of six physical conditions modeled from the restricted Kepler Two-Body Problem (K2BP). They were [12]:

1. The Earth and the spacecraft in question are an isolated system (i.e., we do not consider forces from objects such as the moon).
2. Gravity is exactly Newtonian (i.e., we do not take general relativity into account).
3. No forces other than gravity are exchanged between Earth and the spacecraft.
4. Earth's center is inertially fixed (i.e., the Earth's mass is so large compared to that of the spacecraft that gravitational effects of the spacecraft on Earth are ignored).
5. Earth is spherical and homogeneous (i.e., there are no gravitational perturbations).
6. The spacecraft is a point mass.

These were outlined as simplifications of the problem, so an analytical solution could be approached without rigor. After the establishment of a baseline solution, complications for increased accuracy, such as gravity perturbations due to Earth's non-spherical shape, and influences of the sun and moon could be added.

2.2 Orbital Elements

Before enumerating the definitions of how to look at an orbit, the use of an Earth centered, inertial reference frame is stated. This means that coordinates are centered at the center of Earth, which is assumed to be perfectly spherical and uniform density, and that neither the Earth nor any of the points in the system are accelerating. Again, this is a deviation from real life for ease of understanding and building a model without errors. Afterwards, complexities

for when more accurate applications are required can be added. The positive x-axis points toward the First Point of Aries, which is also the direction of Earth's March equinox. The positive z-axis, a right angle to x-axis, lies along the same direction as a line from Earth's center through its approximate north pole. Finally, the y-axis is at right angles to both and keeping with the right hand rule. An orbit around Earth can be completely described by a set of five parameters, usually referred to as elements. A sixth is usually included referencing a spacecraft's position on that orbit. In a plane, any orbit without a reference frame can be described as an ellipse with an eccentricity, e, and a semi-major axis, a. If the reference frame is centered at one of the focal points, Earth's center, is added, Euler angles are the best way to describe all the possible rotations of an ellipse, a two dimensional shape, about three axes, which can position it in any orientation in three dimensions. The first rotation is the inclination, i, which is the angle between the positive z-axis and the positive angular momentum vector defined as, $\underline{h}$ [13],

$$\underline{h} = \underline{r} \times \underline{v} \tag{2.1}$$

where $\underline{r}$ is the radius vector indicating position of the spacecraft and $\underline{v}$ is the velocity (first time derivative of r, or $\dot{r}$) vector. The second rotation is the right ascension of the ascending node, Ω, which is the angle, measured counter-clockwise when looking down on the xy-plane, between the positive x-axis and the line formed by the intersection of the orbital plane and the equatorial plane. Notice there are two options here and we choose the line, which the spacecraft will travel from south to north (ascending) through the equatorial plane. Also, notice there is a potential discontinuity or an undefined Ω if there is no inclination. Without inclination, the ascending node position becomes arbitrary and we say it is zero and lies along the x-axis so the third rotation has meaning. The third rotation is the argument of perigee, ω, which is the angle between the line of periapsis and the line of the ascending node. Now that the orbit has been precisely described, the final element will show a position on the orbit and is going to be some way to measure time. It can actually be time, t, but more often it is some type of anomaly, an angle the spacecraft is around the orbit away from periapsis. True anomaly, f, mean anomaly, M, and the eccentric anomaly, E, are all used. See Figure 2.1.

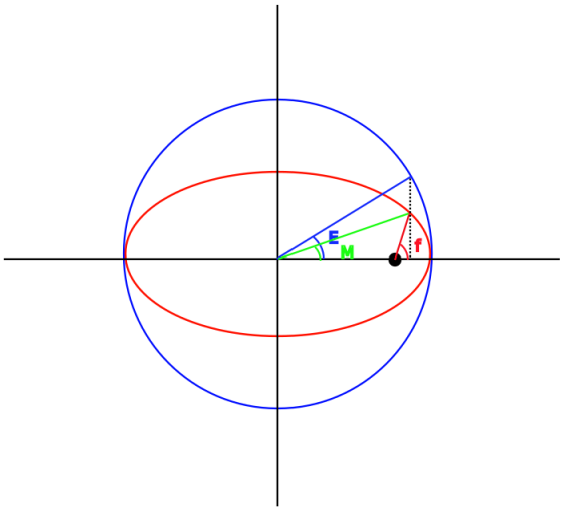

Figure 2.1. True (f), Mean (M) and Eccentric (E) Anomalies

Now that we have all six elements, known as Classical Orbital Elements (COE), spend time on Figure 2.2 for a full understanding.

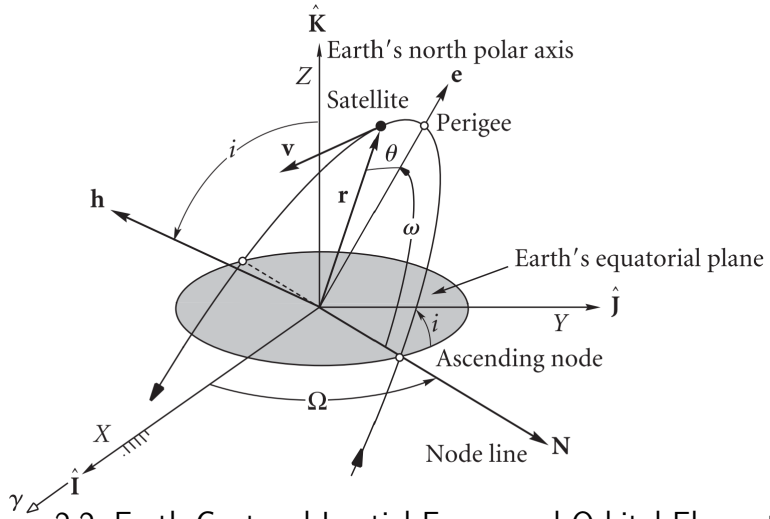

Figure 2.2. Earth-Centered Inertial Frame and Orbital Elements
Source [13].

The common ways to describe an orbit have been outlined thus far. Note that only six pieces of independent data are needed to determine a unique orbit and a spacecraft's position in it. Besides the COE, another common way is using the Cartesian position and velocity vectors of a spacecraft with respect to an Earth-fixed inertial reference frame. The six parameters in that case are the distance and velocity components in three orthogonal bases. Since each set of six parameters can uniquely define an orbit and a position, they can also be converted from one set to any other. Continued next is the development of equations of motion, which all future algorithms were based.

2.3 Equations of Motion

Starting with Newton's Second Law of Dynamics [14],

$$F = ma, \tag{2.2}$$

it is set equal to Newton's Law of Universal Gravitation [14],

$$F = G\frac{m_1 m_2}{r^2}. \tag{2.3}$$

Focusing on the force experienced by the spacecraft, represented by mass m_2, it follows that

$$m_2 a_2 = F_2 = F = G\frac{m_1 m_2}{r^2}. \tag{2.4}$$

Focusing on the outer terms and dividing by m_2, it follows that

$$a_2 = G\frac{m_1}{r^2}. \tag{2.5}$$

Since these are magnitudes and the acceleration is acting in the direction of the origin in the reference frame, direction is implied by adding a unit vector along this direction, $\frac{\underline{r}}{r}$, and relate a_2 as the second time-derivative of r [12], it follows that

$$\ddot{\underline{r}} = G\frac{m_1 \underline{r}}{r^3}. \tag{2.6}$$

The use of dots is to signify derivatives with respect to time and underlines to signify vectors. Finally, combining the universal gravitational constant, G, and the mass of the Earth, m_1,

for
$\mu = 3.986004415e14\ m^3/s^2$ [15] gives

$$\ddot{\underline{r}} = \frac{\mu \underline{r}}{r^3}. \tag{2.7}$$

This completely integrable equation is extremely powerful and evidence of the need for the assumptions so far. This relationship between current position and acceleration enables the prediction of all future states.

Now, an added control to the system was considered. Adding a force is one way to introduce a control. Here, the problem of minimum change in velocity required, or minimum delta-v (Δv), which is a corollary for minimum fuel, was the focus. Therefore, adding the ability to change the velocity of a spacecraft or imparting a Δv will be the control. Ways of using the precious resource of fuel is examined in the next chapter.

THIS PAGE INTENTIONALLY LEFT BLANK

CHAPTER 3:
Maneuver Development

Difficulty in the outlined problem lies in the complexity of analytical solutions and the inability to derive a closed-form solution, which could be coded into an algorithm. Also, when numerical approximations are achieved, it is only through intense computational power. The research started with basic maneuvers, which could be proven analytically and evolved into the application of numerical approximations. Here is an overview of options used for comparison.

3.1 Impulsive Maneuvers

This thesis focused on impulsive maneuvers, meaning a change to a spacecraft's velocity can be made instantaneously. This focus is dedicated to the practical application of an on-orbit servicing vehicle. The assumption was this type of vehicle would have onboard rocket engines that could transfer forms of energy very quickly (i.e., the energy stored in bonds between atoms transferred to directed molecule velocity). This would be the only orbital maneuver option due to the mission. These high thrust burns would be favored over low thrust during potential on-orbit servicing missions since they save time, one of the most valuable resources. It also simplifies computational time since only two major burn calculations would be needed instead of a numerical approximation of an continuous thrust maneuver. The relationship between the other most important resource mass, with potential Δv is [13]

$$\frac{\Delta m}{m} = 1 - e^{-\frac{\Delta v}{I_{sp} g_o}}. \tag{3.1}$$

When examining this equation, note that m (the initial mass of spacecraft before an impulsive burn), I_{sp} (the specific impulse of the engine), and g_o (Earth's gravitational constant at the Earth's surface) are all constants. The only variables to consider are the change in mass (the amount of fuel burned and expelled) and the change in velocity. This relationship shows engineers potential areas of focus in designing an on-orbit servicing satellite when the mission calls for the highest level of Δv possible. Specifically, the closer Δm to m that could be achieved, the better. Note, that m would include target spacecraft, if it was a "space tug"

mission – to change the target's orbit by applying Δv after the OOS spacecraft attached itself to the target. That would mean the servicing spacecraft would need to be much larger than the serviced to reduce the effect the target's mass would have on the ratio, $\frac{\Delta m}{m}$. The other key in design is in I_{sp}. The more efficient use of fuel and engine combination can increase the available Δv.

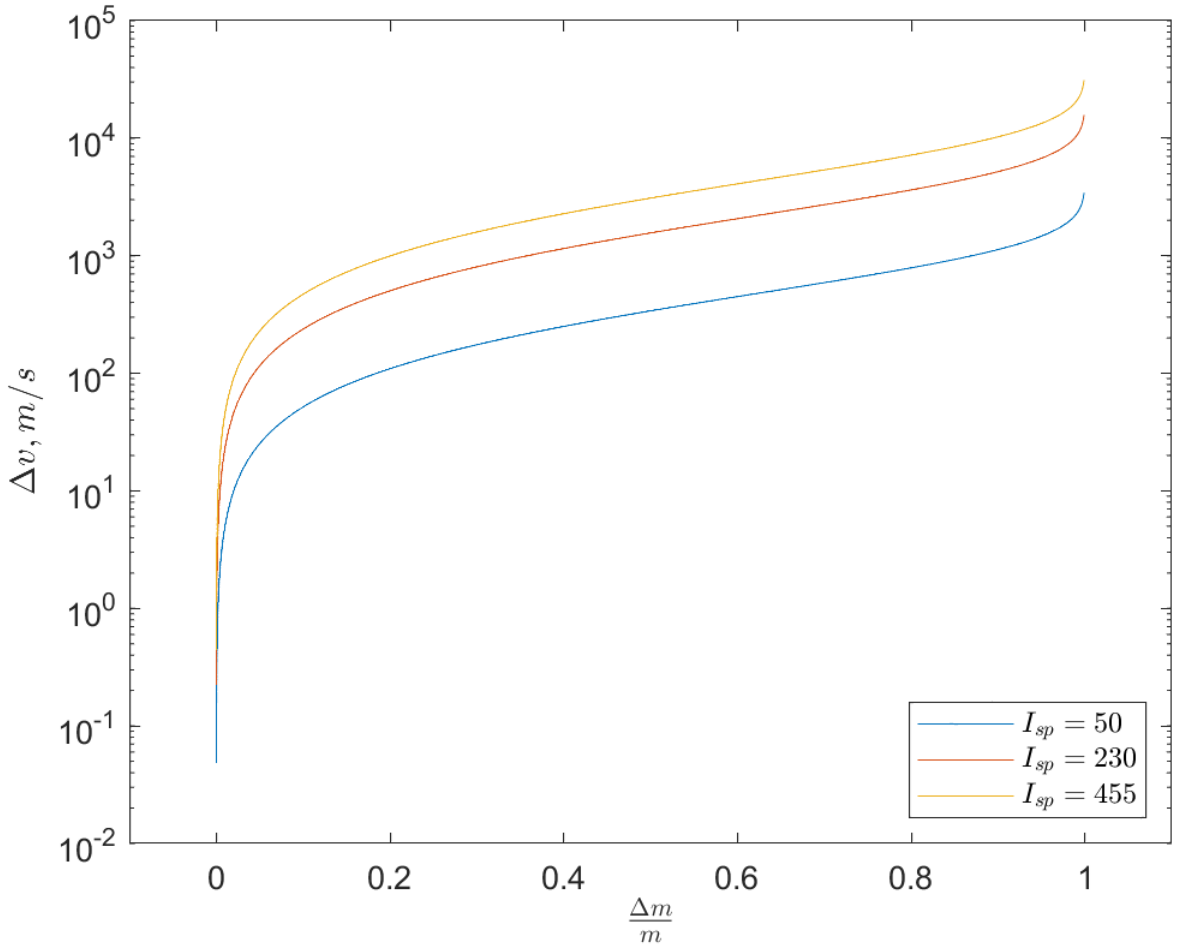

Figure 3.1. Varying Δv and I_{sp} vs. $\frac{\Delta m}{m}$

Here is a summary of Δv and how the effects of I_{sp} and $\frac{\Delta m}{m}$ should influence design. The I_{sp}s listed are some of the common choices. The blue, red, and yellow lines show typical I_{sp}s for cold gas, monopropellant hydrazine, and liquid oxygen/liquid hydrogen, respectively. A materials engineering team that can push $\frac{\Delta m}{m}$ close to 1 would be highly valuable. Adapted from [13].

Note that even with the great I_{sp} of hydrogen and oxygen, to go from a retrograde orbit to prograde orbit (or vice versa) would require such a large Δv, even for the slowest practical orbits, an OOS spacecraft would have to be 75% fuel by mass. Perhaps not impossible for a single maneuver, but considering the mission would be to bring fuel or replacement parts to a target these radical changes are impractical. Similarly, an optimal route determined for an OOS spacecraft would likely group clients of similar inclinations together, due to the high Δv required for plane change maneuvers, evident in the results produced in Chapter 5.

3.2 Hohmann Transfer

The Hohmann Transfer, Figure 3.2, is the well-known optimal transfer between two coplanar circular orbits [13]. This is a type of bi-impulsive rendezvous maneuver that was coded in MATLAB to compare other algorithms for a case with a known solution. This code followed the following logic:

1. Given semi-major axes of two circular orbits, find velocities of a spacecraft on both orbits.
2. Find the eccentricity of an elliptical orbit traveling from one to the other in which its periapsis and apoapsis are tangent to the circles and Earth is still one of its foci.
3. Find the velocities required at periapsis and apoapsis of the transfer orbit.
4. Calculated the Δvs required for entering transfer orbit and leaving the transfer orbit.
5. Sum both Δvs.

The bi-elliptical Hohmann transfer was not considered since it is a three-impulse burn maneuver. It is also impractical in most scenarios, since the ratio of target semi-major axis to chaser semi-major axis needs to be greater than 11.94 to be worth considering [13].

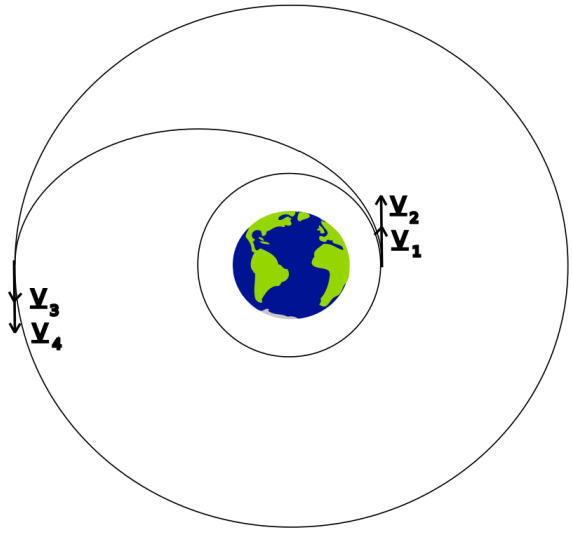

Figure 3.2. Hohmann Transfer

Not to Scale.

3.3 Phasing Maneuvers

One of the most common movements a servicing satellite might encounter is changing just its anomaly at a different rate than happens naturally in the orbit. That is, if a chaser were in the same orbit as its target, it could go to a higher or lower orbit to slow down or speed up in order to catch up to the target or let the target catch up to it. This idea is shown in Figure 3.3.

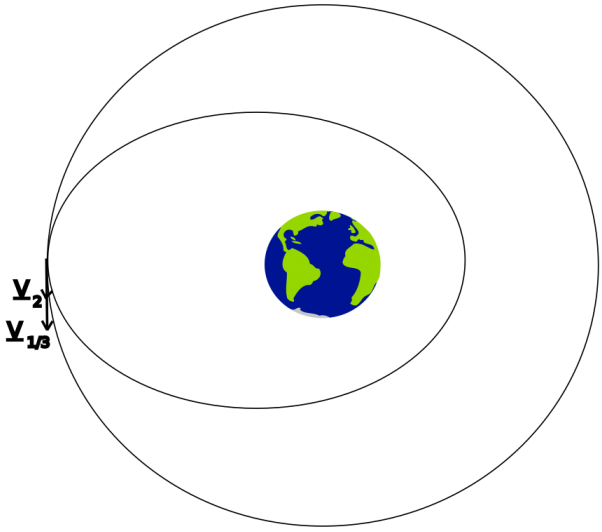

Figure 3.3. Phasing Maneuver

Not to Scale. Start with $\underline{v}_1$. Slow down option shown here. Slow to $\underline{v}_2$. Pass an integer number of orbits before reinsertion. Speed back up to $\underline{v}_3$, which is equal to $\underline{v}_1$. This would allow you to jump ahead or behind in the initial orbit.

The main idea here echoes the periodicity argument in Chapter 4, section 1. The choice of the phasing orbit affects the maneuver time. If the difference in the chaser and target true anomalies were known, the time shift that needs to occur could be calculated. Then, using equation 4.1, it would be a matter of weighing cost of fuel against cost of time. The larger the shift in semi-major axis, the faster the spacecraft could phase, but more fuel would be burned. Periodicity would be a factor because the chaser would be required to enter and leave the orbit at the same location to make use of the efficiency. So, if the chaser orbit period were changed by a measure Δt, then the chaser could reinsert itself into the original orbit after an integer, n, revolutions in the phasing orbit to shift its relative time to the target by $n\Delta t$. For example, say the chaser were behind and the required Δt was 1,500 s to catch up, and among the infinite choices were lowering to two different orbits, one offering a Δt of 100 s and one 300 s per revolution, then, it would take 15 or 5 revolutions, depending on choice. This relationship wouldn't be linear for fuel expenditure, however. In this case, where a 600 km altitude circular orbit was chosen, dropping to 540 km and 357 km orbits

would allow the choices but there would be 4 times the Δv required for the 3 fold decrease in time.

3.4 Plane Change

One way to change an orbit without changing its total energy is changing its plane only. Geometrically, a single burn plane change can be shown to be vector subtraction. See Figure 3.4.

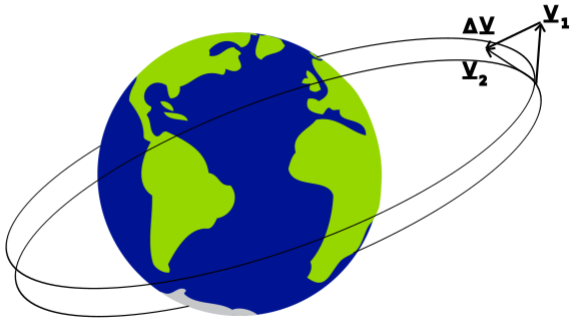

Figure 3.4. Plane Change

In this case, the magnitudes of $\underline{v}_1$ and $\underline{v}_2$ remain equal. Immediately evident is that a π radians change, would require a Δv of $2\underline{v}_1$. Due to the law of cosines, algebraically it would follow

$$\Delta v = \sqrt{\underline{v}_1^2 + \underline{v}_2^2 - 2\underline{v}_1\underline{v}_2 \cos\gamma} \tag{3.2}$$

becomes

$$\Delta v = \sqrt{2\underline{v}_1^2 - 2\underline{v}_1^2 \cos\gamma}, \tag{3.3}$$

which finally becomes

$$\Delta v = \sqrt{2\underline{v}_1^2(1 - \cos\gamma)}. \tag{3.4}$$

This produces evidence that it would be best to do the plane change when the spacecraft is moving slowest in its orbit, the apoapsis. Combining this with the possible magnitude

of a large plane change reveals a narrow inclination window must be imposed for planned serviced spacecraft.

3.5 Lambert's Problem

The general Lambert's problem is when given two points in space around Earth and a time to travel from one to the other, determine the transfer orbit between them [13]. It follows, there are only three variables:

1. $\underline{r}_d$, the position vector of the deputy
2. $\underline{r}_c$, the position vector of the chief
3. Time to travel between deputy and chief.

There are many situations that can narrow the scope of an orbit maneuver. Focus can be on varying one of the orbital elements while keeping the rest the same. Many cases fall into a group such as coplanar changes with or without a common apse line. MATLAB code was developed for these, but not implemented in an optimal solution algorithm.

In this section, generality is searched for through the solving of Lambert's problem. Derived from this solution, the Δv required to change to the transfer orbit from the chaser's orbit could be found, Δv_1, along with the Δv required to shift from the transfer orbit to the final orbit, Δv_2. See Figure 3.5 for an overview of Lambert's problem with Δv calculations.

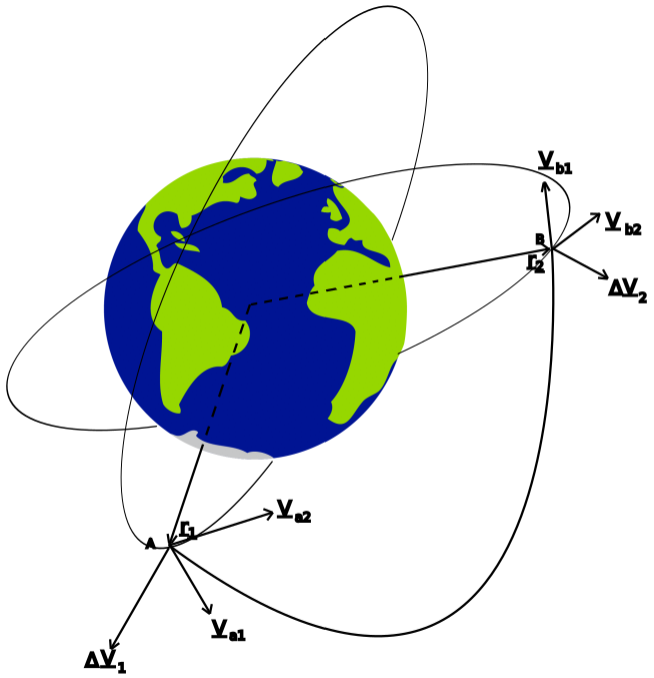

Figure 3.5. Lambert's Problem

Lambert's Problem between orbits around Earth with radius and velocity vectors. We solve the maneuver from point A on orbit 1 to point B on orbit 2 through a transfer orbit with associated $\Delta \underline{v}_{1,2}$.

Combining both of these Δvs we get our total Δv, the cost function seen in equation 3.5. Lambert's algorithm does not solve the issue of a moving target, so in order to implement a rendezvous, the time being considered for transfer must be used to propagate the target spacecraft forward, which serves as the actual target location for solution. This becomes cumbersome when trying to search for an optimal solution. If done properly, however, the three variables for the Lambert problem can be tested as follows:

1. $\underline{r}_d$ is varied by small true anomaly intervals of the deputy's orbit.
2. $\underline{r}_c$ is varied by small true anomaly intervals of the chief's orbit.
3. Time to travel between deputy and chief is varied based on periods of both orbits.

3.6 Minimum ΔV Lambert's Problem

Intuition dictates that a solution method involves developing a model for a deputy and chief and simulating forward progress of time, then comparing all rendezvous options available after each time step. This does not guarantee all possible scenarios in a reasonable time, however (see section 4.1). Instead, computational time could be reduced by comparing chosen intervals of each orbit and varying transit time. These potential launch points could be achieved by just waiting (assuming their periods differed) or by phasing (see section 3.3), changing the rendezvous problem to a four-impulse burn (two for phasing, two for Lambert's transfer). Meaning, once a quasi-optimal solution can be found between orbits through many solutions to Lambert's problem, waiting or lining up the relative positions to start that maneuver could be accomplished with relatively low Δv. A MATLAB code was written by the author to implement a solution to Lambert's problem, and compare solutions. The code was derived from [13]. It follows that minimizing Lambert's problem is a direct search method varying as many (i.e., fine) combinations as willing, which increases computational time and gives more accurate results. The remaining algorithms presented attempt analytical simplifications and search algorithms to solve the problem faster.

3.7 Minimum ΔV^2 Lambert's Problem

Computationally demanding lists of solutions to Lambert's problem is the baseline solution strategy taken for a single jump. The cost function typically is

$$\Delta v = \Delta v_1 + \Delta v_2. \tag{3.5}$$

where Δv_1 and Δv_2 are the magnitudes of $\Delta \underline{v}_1$ and $\Delta \underline{v}_2$ from Figure 3.5. That is, this is the equation that, if could be minimized, would give the optimum minimum fuel maneuver between two arbitrary elliptical orbits, considering any combination of $\underline{r}_c$ and $\underline{r}_d$. However, there is no easy method of analytically minimizing this or bounding it.

Reference [16] proposed a method to identify an approximate optimal transfer between two arbitrary orbits. This was done by minimizing Δv^2, instead, where the goal was to manipulate the new cost function to reduce it to terms of h, the angular momentum, which could be solved for since the first derivative of which proved continuous and could be set to

zero to find possible global extrema. The cost function to be minimized here was

$$\Delta v_{est} = \sqrt{\Delta v_1^2 + \Delta v_2^2}, \tag{3.6}$$

which was rewritten as

$$\Delta v_{est}^2 = C - 2(\underline{v}_{a1} \cdot \underline{v}_{a2} + \underline{v}_{b1} \cdot \underline{v}_{b2}) - \frac{2\mu}{a}. \tag{3.7}$$

C contains only constants of both orbits. In order to minimize Equation 3.7, C was removed with the focus being to maximize what is subtracted from this constant to get Δv^2. The derivative of all non-constant terms was then set to zero and reduced to

$$F(h) = h^4 + c_3 h^3 + c_1 h + c_0 = 0. \tag{3.8}$$

This quartic equation was solved revealing four roots, all possible options for the optimal h of the transfer orbit. Since negative and complex roots have no meaning for h, those were discarded. Two of the four roots would always be discarded [16]. The remaining two roots would be the optimal hs for prograde and retrograde transfer orbit options. This proved an analytical solution for Δv^2 and here these two options were compared, the better one selected and used as a quasi-optimal solution for Δv. A MATLAB code was generated by Riccardo Apa to replicate this process of minimizing Δv^2 and computing the Δv using the h options found.

Note the potential for deviation possible in minimizing Δv versus Δv^2 by squaring both sides of Equations 3.5 and 3.6, it follows

$$\Delta v^2 = \Delta v_1^2 + \Delta v_2^2 + 2\Delta v_1 \Delta v_2, \tag{3.9}$$

which becomes

$$\Delta v_{est}^2 = \Delta v_1^2 + \Delta v_2^2. \tag{3.10}$$

Since Δv_1 , $\Delta v_2 \geq 0$,then $\Delta v_{est} \leq \Delta v$. Due to Young's inequality,

$$\Delta v^2 = \Delta v_1^2 + \Delta v_2^2 + 2\Delta v_1 \Delta v_2 \leq \Delta v_1^2 + \Delta v_2^2 + \Delta v_1^2 + \Delta v_2^2 = 2\Delta v_{est}^2. \tag{3.11}$$

Square root both sides shows $\Delta v \leq \sqrt{2}\Delta v_{est}$. Now Δv is bounded on both sides in terms of Δv_{est}, as in

$$\Delta v_{est} \leq \Delta v \leq \sqrt{2}\Delta v_{est}. \tag{3.12}$$

Here, Δv is the optimal solution to minimizing Equation 3.5, to which there is no analytical algorithm yet developed, and Δv_{est} is what can be calculated using the base Equations 3.7 and 3.8, with solutions to the first derivative test providing options for h for the transfer orbit which gives a minimum Δv^2.

3.8 Primer Vector Method

The primer vector, first introduced by Lawden [17], uses variational calculus to optimize impulsive thrust rendezvous trajectories. The trivial case is the bi-impulsive case studied here. A MATLAB code [18] that uses this method to ensure optimality of Δvs was added to the algorithms compared. Although the full solution is beyond the scope of this thesis, this method can be broken down into three distinct sections.

First, an analytical representation of change in Δv with respect to the semi-latus rectum of the transfer orbit, p was found with bounds on p. To which, Brent's root-finding method (e.i., a combination of the bisection method, secant method, and inverse quadratic interpolation) found possible solutions [19].

Second, an additional direct search algorithm was applied to these solutions across potential positions and velocities on both orbits. MATLAB's $fminsearch$ was used to apply the Nelder-Mead algorithm, searching which relative positions revealed minimum Δv, while drastically reducing the set of test locations required [20].

Finally, primer vector theory was used to determine if a found solution was an optimal solution. This was done by setting the primer equal to the direction of thrust, or the change in $\underline{r}$ with respect to $\underline{r}_o$ and $\underline{v}_o$ [18], [17].

Although, intuition would loop these one inside the other, $fminsearch$ reduced most of the work that would be required by an exhaustive list of results from Brent's root-finding loop by determining which inputs to drop into Brent's method and comparing them. This is the basis of the Nelder-Mead method, where a set of sets (i.e., a simplex) of positions and

velocities were compared in varying ways to determine the next simplex, until there was a simplex that had no way to maneuver any set within to get a better result [20]. Then, the result was finally checked against the associated primer vectors for optimality.

CHAPTER 4:
Considerations

Operators will have many options when choosing maneuvers for their satellites. This chapter highlights two of the most important factors when making that choice.

4.1 Relative Periodicity

When faced with the problem of changing from one orbit to another with a different semi-major axis, there will be a measure of time until the chosen maneuver can take place, then a repeating interval of time where the same maneuver can happen. This is due to the relative positions of deputy and chief orbits changing in a predictable repetitive way. The coplanar, Circular to Circular (C2C) case shows this idea in its simplest case. A common example is a trip from Earth to Mars, in which the ideal maneuver opportunity happens every 26 months, approximately [21].

In order to bound the time search interval for a transfer between two satellites, a MATLAB code was written to determine the relative period between two orbiting objects. The code looks at two arbitrary orbits and relative position between deputy and chief locations. It takes as inputs these locations as well as a tolerance of how close the positions should be to still be considered the chosen maneuver's required starting orientation. So, assumed here was that the chosen maneuver starts at known COE for the deputy and chief locations.

The known solution of the synodic period between Earth and Mars was used to validate the code. The common assumptions of Earth and Mars both having a circular orbit around the sun and are coplanar were imposed on the code, which was developed for any aribitrary orbit around Earth. A few small changes in the code to allow for this comparison are:

1. Converting the geocentric gravitational constant to the heliocentric gravitational constant
2. Increasing accuracy parameter of minimizing norms
3. Increasing the step size of testing times
4. Changing accuracy parameter from comparing vector to comparing vector length

The first three changes are intuitive. The last was a simplification due to coplanar, circular return to exact conditions does not require a specific launch point, just a specific orientation. This reduced the problem to a basic synodic period problem.

Narrowing the difference in the vector magnitude between the starting positions and final positions of Earth and Mars in the code to 2.683 Kilometers (km), checking once per day for the time step, the numerical result for the interval of time for repeating relative positions was 26.03 months. Decreasing the accuracy of the vector magnitude decreased the interval of time. For instance, better than 1 million km resulted in 25.77 months for the time interval. So, this type of code would not only provide the decision-maker with an accurate time frame, but an understanding of the sensitivity to numerical tolerances.

Shown in Figure 4.1 is a brief deductive proof of the coplanar, circular synodic problem between Earth and Mars.

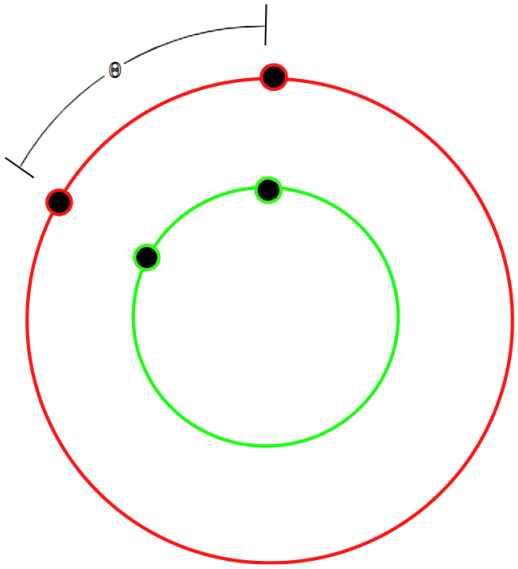

Figure 4.1. Traveling an Angle, θ

The Mars path in red would travel θ or $2\pi n + \theta$, whereas the Earth path would travel $2\pi m + \theta$, depending on proportional difference in periods. $(m, n \in \mathbf{N})$

Observe the period function with a as the semi-major axis and τ as the period [12], as in

$$\tau^2 = \frac{4\pi^2 a^3}{\mu}. \tag{4.1}$$

Then, when comparing two orbits, the one with a smaller semi-major axis must have a shorter period. Corollary, the smaller also has a faster angular velocity, as seen in Equation 4.3. Due to the radial symmetry of circles, whichever starting points the two planets (or satellites) have, both must travel the same final angle, θ. The only difference is, the smaller orbit, having the faster angular velocity, must travel an integer ≥ 1 number of orbits to align with the outer orbit. The smaller orbit's fastest option would be 1 orbit or $2\pi + \theta$ radians being the fastest next possible alignment. Assuming the best relative position to initiate travel from Earth to Mars could be known, the synodic period would be the time between this optimal start and the next available optimal start. First, angular velocities were found, as in

$$\omega = \frac{2\pi}{\tau}. \tag{4.2}$$

Substituting equation 4.1 into 4.2, it followed that

$$\omega = \sqrt{\frac{\mu}{a^3}}. \tag{4.3}$$

If ω_E were Earth's angular velocity and ω_M for Mars, and the synodic period, τ_{syn}, then

$$\theta = \omega_M \tau_{syn}, \tag{4.4}$$

and

$$\theta + 2\pi = \omega_E \tau_{syn}. \tag{4.5}$$

Substituting 4.4 into 4.5, τ_{syn} was solved for, as in

$$\tau_{syn} = \frac{2\pi}{\omega_E - \omega_M}. \tag{4.6}$$

With semi-major axis of 227,956,000 km and 149,598,000 km [22] for Mars and Earth, respectively plugged into 4.3 with μ_{sun} of $1.32712442099e20\ m^3/s^2$ [15], it becomes

τ_{syn} = 6.73793e7 Seconds (s) or 25.9951 Months (mo).

This result was in line with the MATLAB code results and a 0.01154% variation within NASA's published results [22].

This idea is crucial to the programmer since it provides a time window where all possible relative positions can be compared. This is one way to vastly reduce the computational power required to determine absolute optimal maneuvers. It also provides a wait time if a desired burn is missed until the exact conditions repeat.

Unfortunately, traveling to or from an elliptical orbit or if the orbits are non-coplanar the symmetry benefit used going from circular to circular can not be applied and the interval to repeat relative positions is vastly increased.

4.2 Variations from Bi-Impulsive

Even though the focus of this study was bi-impulsive rendezvous maneuvers to change orbits, there are unique circumstances that could require planners to investigate other routes, using the same equipment. Consider a large plane change in which the magnitude of Δv is unusually high. There are ways to reduce this burden. If you consider perturbations, a deviation from the K2BP, there may be a way to use differential node rotation if long wait times are not an issue. However, one of the main underlying assumptions of this thesis was that long wait times would be an issue. So, an option more valuable may be considering more impulses. If this is allowed for, the apogee could be raised, lowering the lowest velocity in orbit, then making the inclination change, then lowering the apogee back. Consider a 600 km by 39,700 km orbit (i.e., perigee and apogee altitudes). Due to the conservation of energy equation [13],

$$\frac{v^2}{2} - \frac{\mu}{r} = -\frac{\mu}{2a}, \tag{4.7}$$

there would be a velocity at apogee of 1.51 km/s. If 0.122 km/s Δv at perigee were added to raise the apogee to 50,000 km, the velocity at apogee would be 1.25 km/s. This means only an inclination change of 0.22 rad would make this three burn worth it compared to the single.

4.3 Traveling Salesman Problem

Mission planning for an on-orbit servicing satellite with many targets is a complex task. This type of problem is commonly referred to as the TSP, which is a specific type of Vehicle Routing Problem (VRP) [9], [10], [11]. Whereas the TSP has traditionally answered how a person would travel the least distance between a list of cities starting and ending at the same place, the VRP is a more general problem, which searches for all the optimal routes associated with a fleet of vehicles to reach all targets fulfilling each target's requirements [23]. So, the TSP is a VRP with one vehicle (a traveling salesman's car), a number of static, deterministic nodes (list of cities), with no node requirements other than the first and last node must be the same. In the orbital TSP, the computing cost to travel between nodes is more complex than a fixed distance. This research was an attempt to reduce the computational time required to achieve a reasonable quasi-optimal fuel solution for an orbit transfer.

Algorithms for reducing a single Δv calculation time could be applied to an exhaustive list of all cost possibilities with reduced integrity of each calculation, but VRP algorithms reduce the exhaustive list needed while keeping the integrity of a single Δv cost. Then, both techniques could certainly be combined after the impact of both are well understood.

Before this section, a way to solve for the optimal minimum fuel maneuver between two arbitrary elliptical orbits within a reasonable time was shown. Unfortunately, solving a TSP between these types of orbits means the positions and velocities of the spacecrafts, and hence the Δv required for rendezvous (corollaries for location and distance in the traditional TSP) are not static. This increases the hardness of the TSP problem, since calculating a list of all possible costs, becomes a permutation problem, where all objects are being chosen out of the total number of objects, reducing the permutation equation to $N!$ possibilities, N being the number of nodes (or clients or cities) that are planned for visit. Each possibility represents a set of N costs that must be calculated. So, stringing multiple jumps together compounds the problem factorially, which can be seen in

Table 4.1. Permutations and Cost Computations Required for Number of Nodes

N	Possibilities	Cost Computations	Total Time, s	N	Possibilities	Cost Computations	Total Time, s
1	1	1	1.67e3	9	3.62e5	3.26e6	5.44e9
2	2	4	6.67e3	10	3.62e6	3.62e7	6.03e10
3	6	18	3.00e4	15	1.31e12	1.97e13	3.29e16
4	24	96	1.60e5	20	2.43e18	4.84e19	8.07e22
5	120	600	1.00e6	25	1.55e25	3.88e26	6.47e29
6	720	4,320	7.20e6	50	3.04e64	1.52e66	2.53e29
7	5,040	3.52e4	5.87e7	100	9.33e157	9.33e159	1.56e163
8	4.03e4	3.22e5	5.37e8	1000	4.02e2567	4.02e2570	6.7e2573

Table 5.6 was used to compute average time per cost computation using Lambert's algorithm to input total times in Table 4.1, – the time projected to solve an N-node TSP on a Microsoft Surface Pro 7 with 16GB of RAM and an Intel Core i7-1065G7 processor. For perspective, the world's fastest supercomputer, the Hewlett Packard Enterprise Frontier can compute 1.6 exaflops (1.6e18 floating point operations per second) [24]. If calculating a single optimal Δv took only 1 flop, the computational time for Frontier to find the optimal route between 25 spacecraft would be 7.69 years or 20 spacecraft in 30.3 seconds. The latter doesn't seem bad, but it becomes an affordability issue. The Frontier was built for $600M [24]. Also, each Δv takes thousands of flops. With that in mind, the Microsoft Pro could use Lambert's algorithm to solve 5 nodes in 11 days, 10 nodes in 1900 years. This thesis was limited by the use of a single Intel Core i7-1065G7 processor. One of the most economical computing options in 2022 was Nvidia's RTX4090, retailing at $1,599 claiming 82.6 teraflops (8.26e13 flops [25]). That would be 1/19,370th of the computing power for only 1/375,235th the cost of the Frontier, but 290x as powerful is the i7-1065G7 and 3x the price. There would still be a large portion of a mission budget dedicated to purchasing hardware just for flight path planning, either way.

CHAPTER 5:
Results

The purpose of this chapter is to present results of increasingly complex orbit transfer cases. The presentation of each case follows:

1. Explain any reasoning behind choices.
2. Show plot of orbits to be tested.
3. Show table of results. Large data sets reduced to single example table.
4. Plot of results. Large data sets reduced to single plot showing major trends.

Consistent with likely limitations imposed on OOS spacecraft missions presented in section 3.1, it was assumed that every orbit was traveling in the same direction (i.e., both deputy and chief were retrograde or they were both prograde).

5.1 Coplanar

5.1.1 C2C

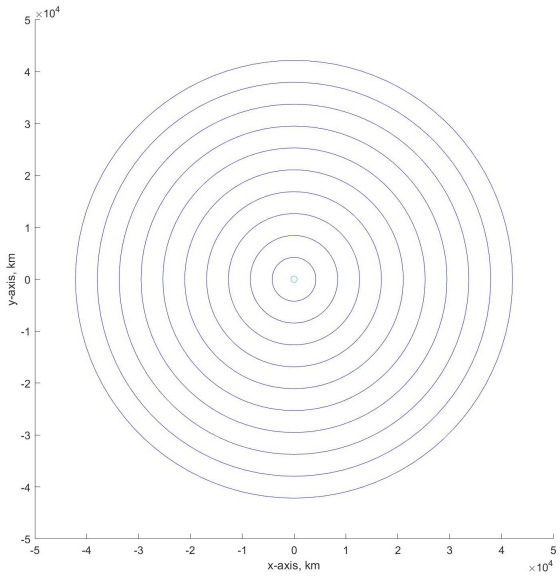

Figure 5.1. Orbits Tested for Coplanar, C2C

Table 5.1. Coplanar, C2C Results

Semi-Major Axis of Deputy, km	Hohmann, km/s(Actual)	Primer Vector km/s,(% deviation)	Minimize Δv^2 km/s,(% deviation)	Lambert km/s,(% deviation)
0.1	5.151088	5.151088(0.00%)	5.150925(0.003%)	5.152534(0.28%)
0.2	3.300136	3.300134(0.00%)	3.299825(0.009%)	3.304146(0.12%)
0.3	2.335039	2.335033(0.00%)	2.334918(0.005%)	2.335417(0.016%)
0.4	1.699533	1.699533(0.00%)	1.699449(0.005%)	1.701964(0.14%)
0.5	1.236884	1.236884(0.00%)	1.236796(0.007%)	1.237757(0.071%)
0.6	0.880447	0.880445(0.00%)	0.880350(0.011%)	0.880586(0.016%)
0.7	0.595542	0.595542(0.00%)	0.595488(0.009%)	0.596687(0.19%)
0.8	0.361790	0.361790(0.00%)	0.361743(0.013%)	0.362299(0.14%)
0.9	0.166201	0.166201(0.00%)	0.166141(0.036%)	0.166282(0.049%)

The accuracy of the primer vector method determined its use as the baseline for all other cases.

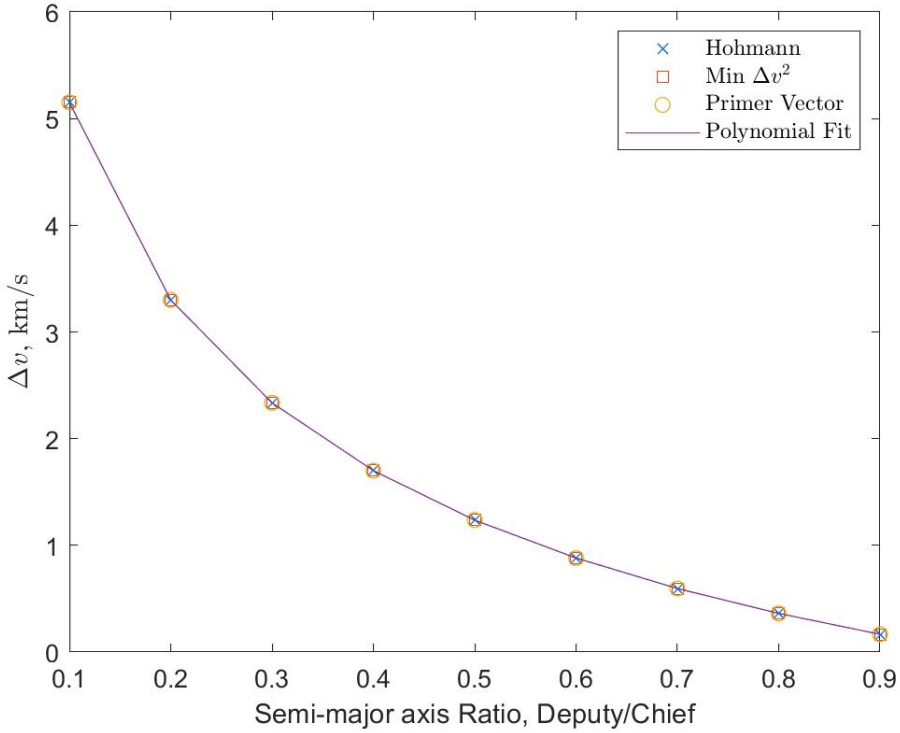

Figure 5.2. Coplanar, C2C Results

Table 5.2. Coplanar, C2C Results, Time

	Hohmann	Primer Vector	Minimize Δv^2	Lambert
Computational time, s	0.005247	103.7	16.14	373.1

Precision for the Lambert code was increased until results in Table 5.1 had less than 0.3% variation.

5.1.2 Circular to Elliptical (C2E)

Two subcases were considered:

1. GEO to GEO, varying eccentricity of chief
2. GEO to LEO, varying eccentricity of chief

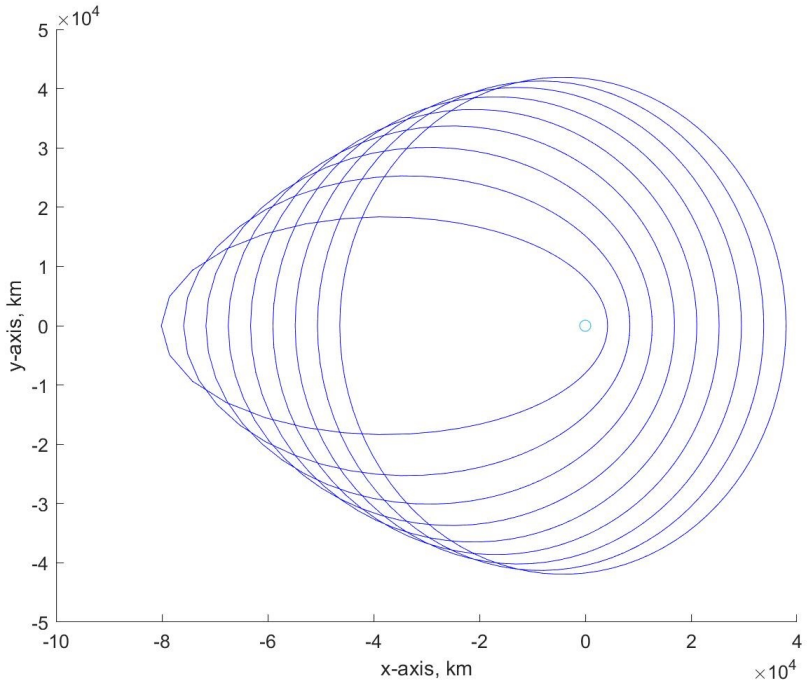

Figure 5.3. Orbits Tested for Coplanar, C2E, GEO to GEO

Table 5.3. Coplanar, C2E, GEO to GEO Results

Eccentricity of Chief, km	Primer Vector km/s (Actual)	Minimize Δv^2 km/s,(% deviation)	Lambert km/s
0.1	0.152134	0.152209(0.049%)	0.152725(0.39%)
0.2	0.302406	0.302519(0.037%)	0.302891(0.16%)
0.3	0.452828	0.452964(0.030%)	0.453593(0.17%)
0.4	0.605657	0.605811(0.025%)	0.606256(0.099%)
0.5	0.763711	0.763870(0.021%)	0.764506(0.10%)
0.6	0.930923	0.931089(0.018%)	0.931205(0.030%)
0.7	1.113578	1.113746(0.015%)	1.113666(0.008%)
0.8	1.323636	1.323808(0.013%)	1.323826(0.014%)
0.9	1.591941	1.592111(0.011%)	1.592477(0.033%)

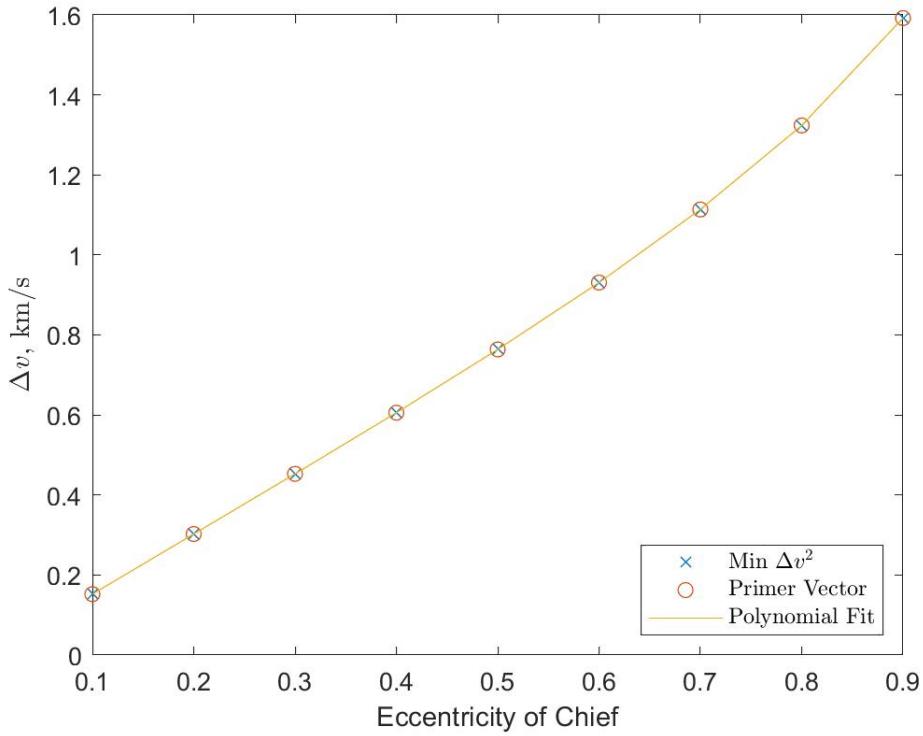

Figure 5.4. Coplanar, C2E, GEO to GEO Results

Table 5.4. Coplanar, C2E, GEO to GEO Results, Time

	Primer Vector	Minimize Δv^2	Lambert
Computational time, s	103.9	16.4	378.3

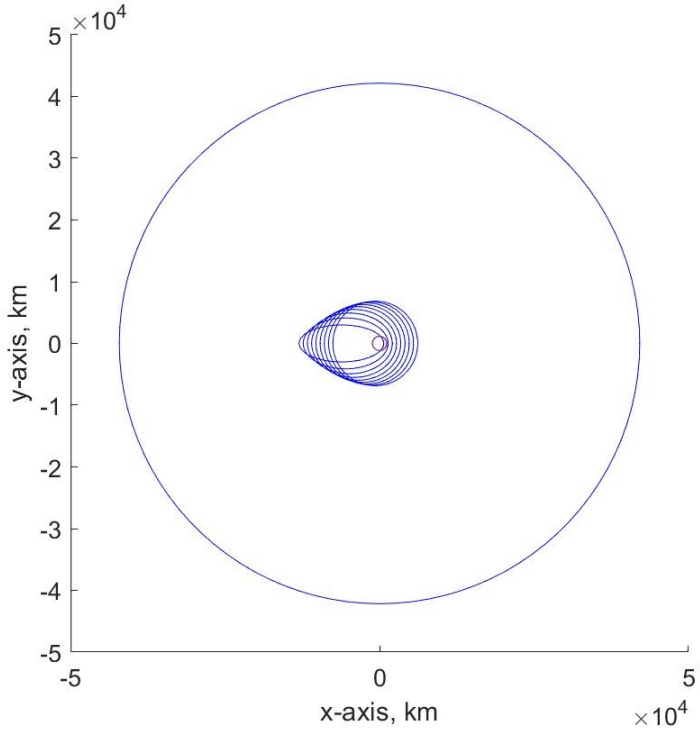

Figure 5.5. Orbits Tested for Coplanar, C2E, GEO to LEO

Table 5.5. Coplanar, C2E, GEO to LEO Results

Eccentricity of Chief, km	Primer Vector km/s(Actual)	Minimize Δv^2 km/s,(% deviation)	Lambert km/s,(% deviation)
0.1	3.699748	3.700818(0.029%)	3.725433(0.69%)
0.2	3.594347	3.596097(0.049%)	3.607791(0.37%)
0.3	3.498848	3.512540(0.39%)	3.504152(0.15%)
0.4	3.412568	3.427714(0.44%)	3.413569(0.029%)
0.5	3.335015	3.355458(0.61%)	3.334501(0.015%)
0.6	3.265990	3.287161(0.65%)	3.268684(0.082%)
0.7	3.205479	3.231364(0.81%)	3.212876(0.23%)
0.8	3.153761	3.186492(1.0%)	3.168139(0.45%)
0.9	3.111455	3.211736(3.2%)	3.133614(0.71%)

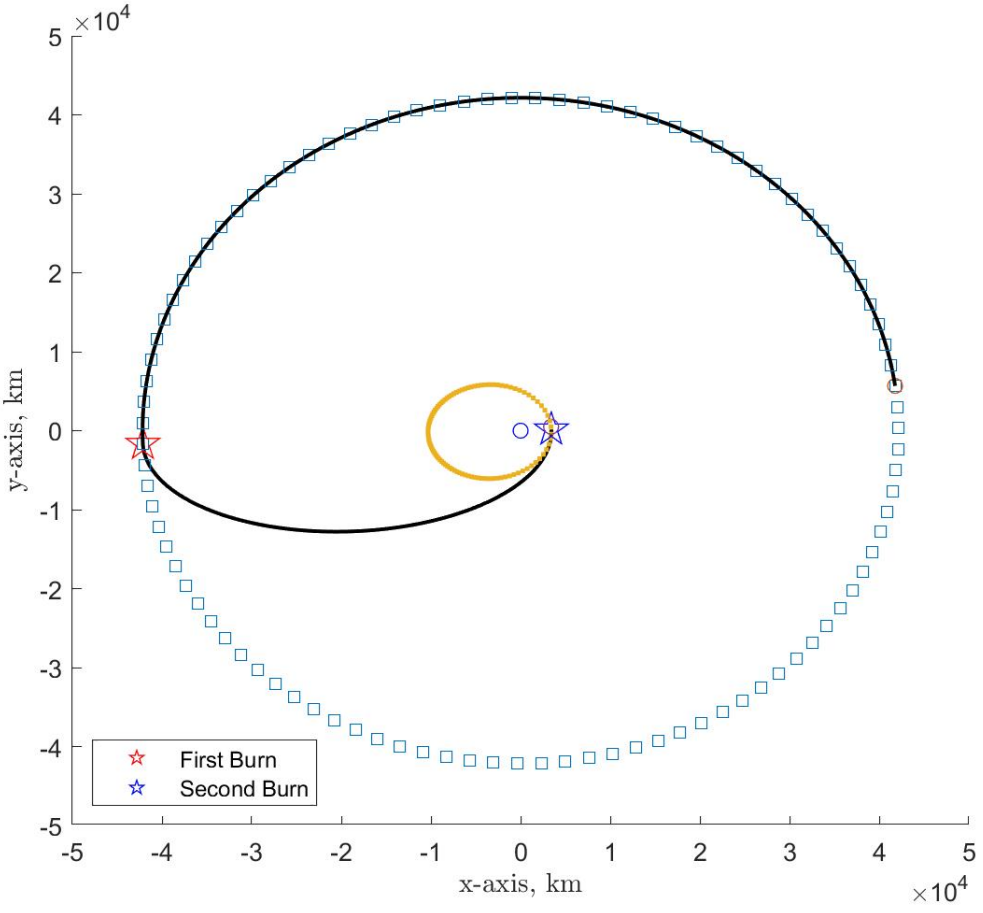

Figure 5.6. Coplanar, C2E, GEO to LEO Example Flight Path

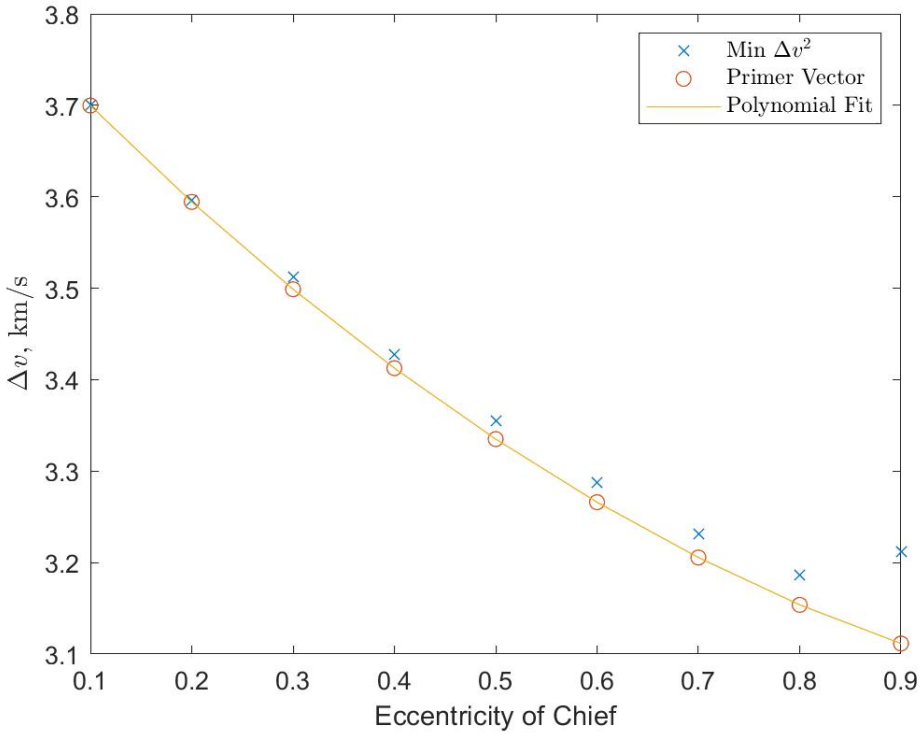

Figure 5.7. Coplanar, C2E, GEO to LEO Results

Table 5.6. Coplanar, C2E, GEO to LEO Results, Time

	Primer Vector	Minimize Δv^2	Lambert
Computational time, s	100.6	17.3	15009.8

5.1.3 Elliptical to Circular (E2C)

Again, two subcases were considered:

1. GEO to GEO, varying eccentricity of deputy

2. LEO to GEO, varying eccentricity of deputy

In other words, these were the reverse cases of section 5.1.2.

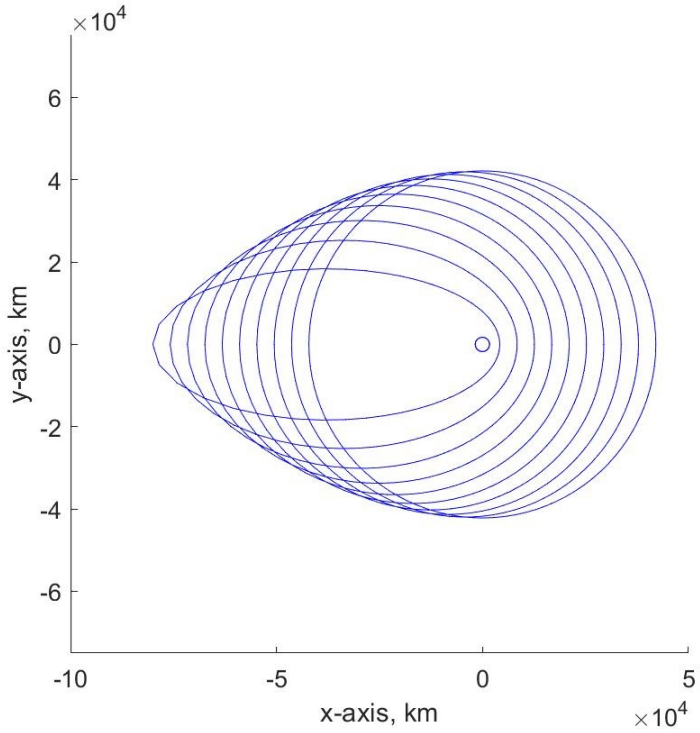

Figure 5.8. Orbits Tested for Coplanar, E2C, GEO to GEO

Table 5.7. Coplanar, E2C, GEO to GEO Results

Eccentricity of Deputy, km	Primer Vector km/s (Actual)	Minimize Δv^2 km/s (% deviation)
0.1	0.152133	0.152209(0.050%)
0.2	0.302406	0.302519(0.037%)
0.3	0.452828	0.452964(0.030%)
0.4	0.605658	0.605811(0.025%)
0.5	0.763711	0.763870(0.021%)
0.6	0.930924	0.931089(0.018%)
0.7	1.113577	1.113746(0.015%)
0.8	1.323636	1.323808(0.013%)
0.9	1.591937	1.592111(0.011%)

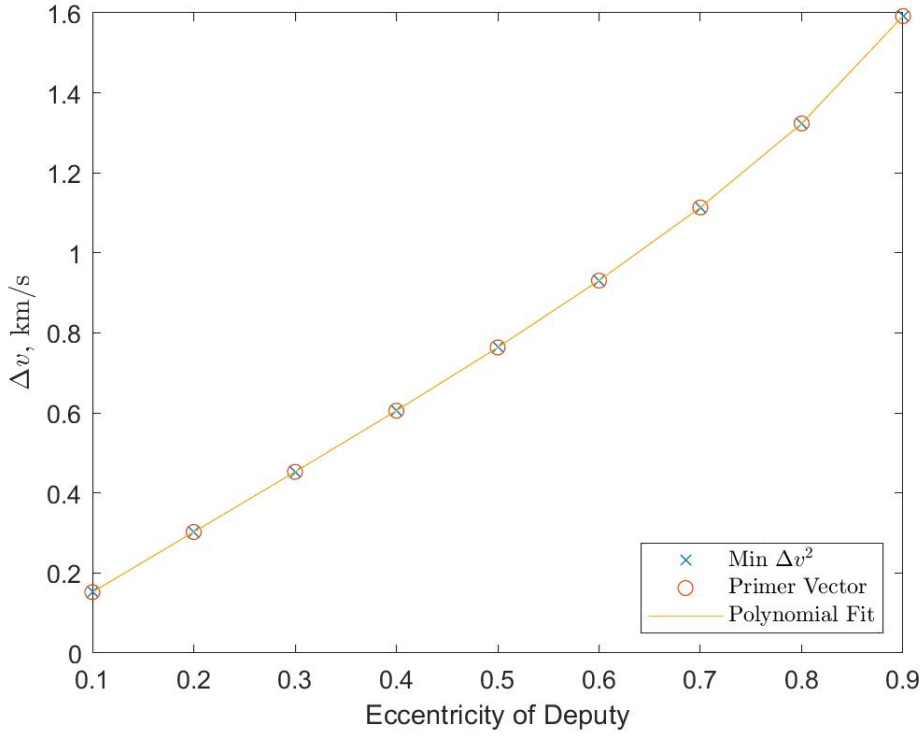

Figure 5.9. Coplanar, E2C, GEO to GEO Results

Table 5.8. Coplanar, E2C, GEO to GEO Results, Time

	Primer Vector km/s	Minimize Δv^2 km/s
Computational time, s	108.5	16.6

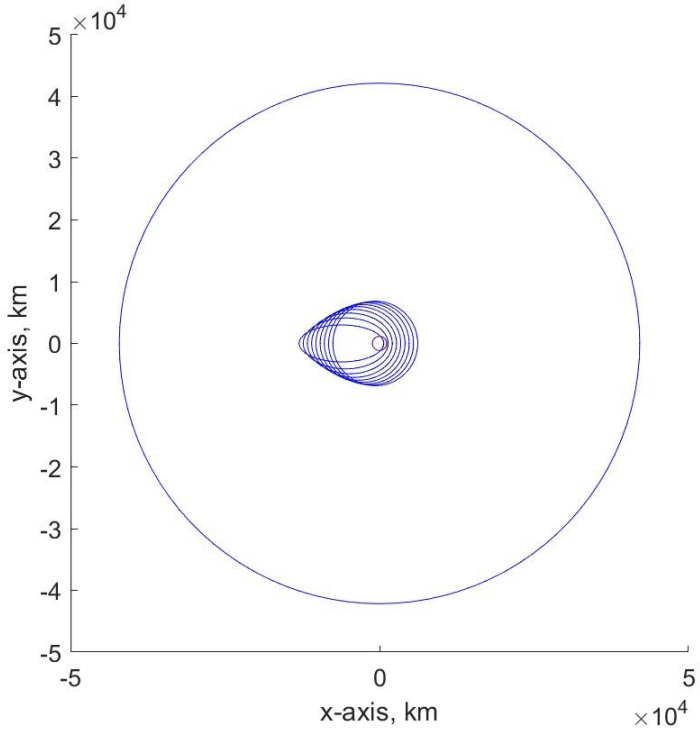

Figure 5.10. Orbits Tested for Coplanar, E2C, LEO to GEO

Table 5.9. Coplanar, E2C, LEO to GEO Results

Eccentricity of Deputy, km	Primer Vector km/s (Actual)	Minimize Δv^2 km/s (% deviation)
0.1	3.699748	3.714281(0.39%)
0.2	3.594347	3.609152(0.41%)
0.3	3.498849	3.516377(0.50%)
0.4	3.412556	3.430440(0.52%)
0.5	3.335015	3.353420(0.55%)
0.6	3.265992	3.296665(0.94%)
0.7	3.205479	3.231599(0.81%)
0.8	3.153760	3.181695(0.89%)
0.9	3.111453	3.166013(1.8%)

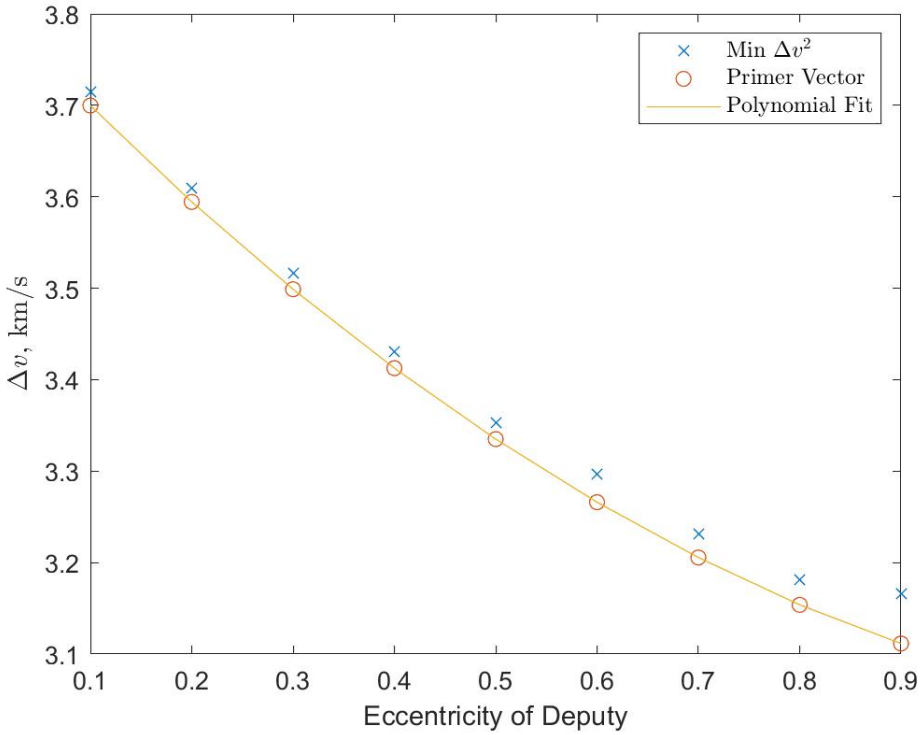

Figure 5.11. Coplanar, E2C, LEO to GEO Results

Table 5.10. Coplanar, E2C, LEO to GEO Results, Time

	Primer Vector km/s	Minimize Δv^2 km/s
Computational time, s	109.5	16.6

5.1.4 Elliptical to Elliptical (E2E) with Common Apse Line

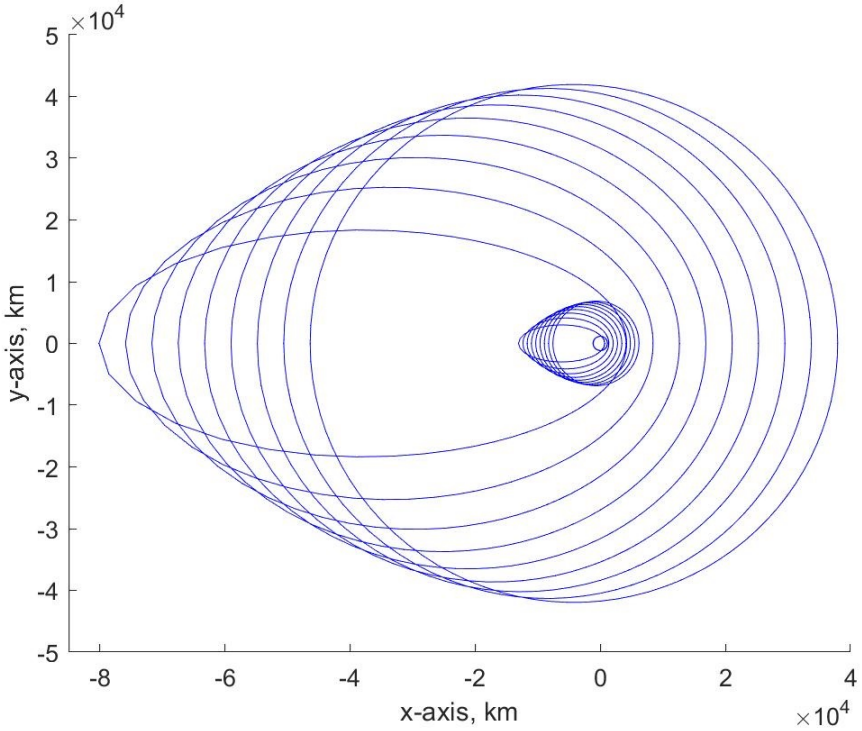

Figure 5.12. Orbits Tested for Coplanar, E2E, LEO to GEO

Table 5.11. Coplanar, E2E, LEO to GEO Results Example

Deputy Eccentricity	Primer Vector km/s e_C=0.1	Minimize Δv^2 km/s e_C=0.1	% Variation , %
0.1	3.601562	3.601693	0.004
0.2	3.495671	3.496111	0.013
0.3	3.382308	3.382528	0.006
0.4	3.260824	3.261005	0.006
0.5	3.129581	3.130017	0.014
0.6	2.985529	2.985816	0.010
0.7	2.823058	2.823521	0.016
0.8	2.630722	2.631499	0.030
0.9	2.657048	2.657974	0.035

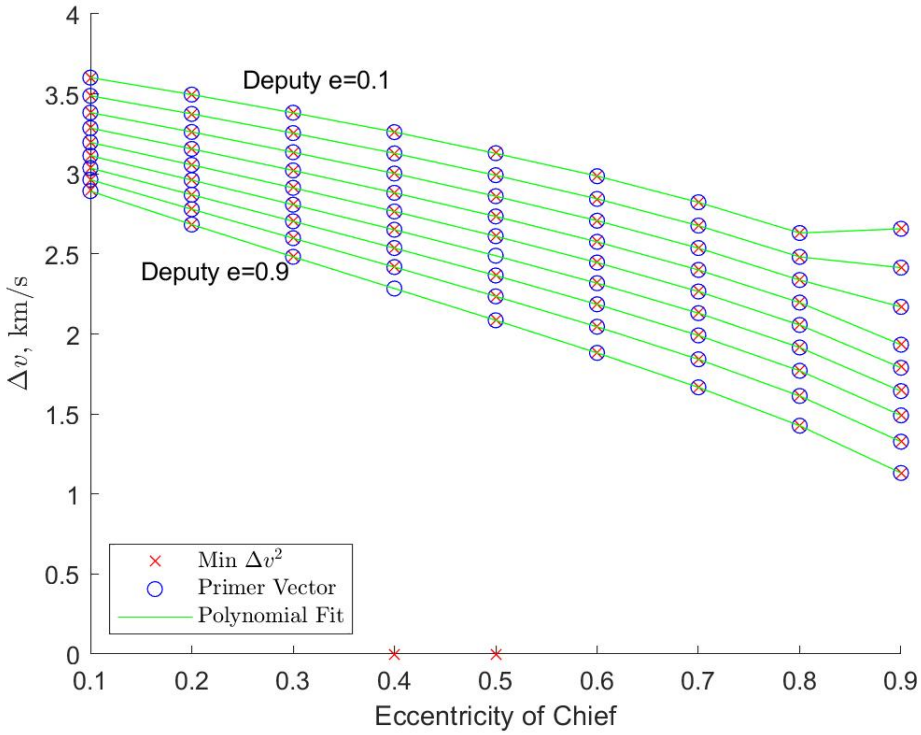

Figure 5.13. Coplanar, E2E, LEO to GEO Results

Table 5.12. Coplanar, E2E, LEO to GEO Results, Time

	Primer Vector km/s	Minimize Δv^2 km/s
Computational time, s	902.7	226.4

5.2 Non-coplanar

5.2.1 C2C

Following the same pattern as coplanar results, C2C was considered the least complex and, hence, the starting point for non-coplanar. a_C and i_C were incremented from a ratio of .1 to 1 by .1 and from 0° to 90° by 10°, respectively. Figure 5.14 first shows varying i_C for a single a_C. Then, Figure 5.15 shows varying i_c for all a_c.

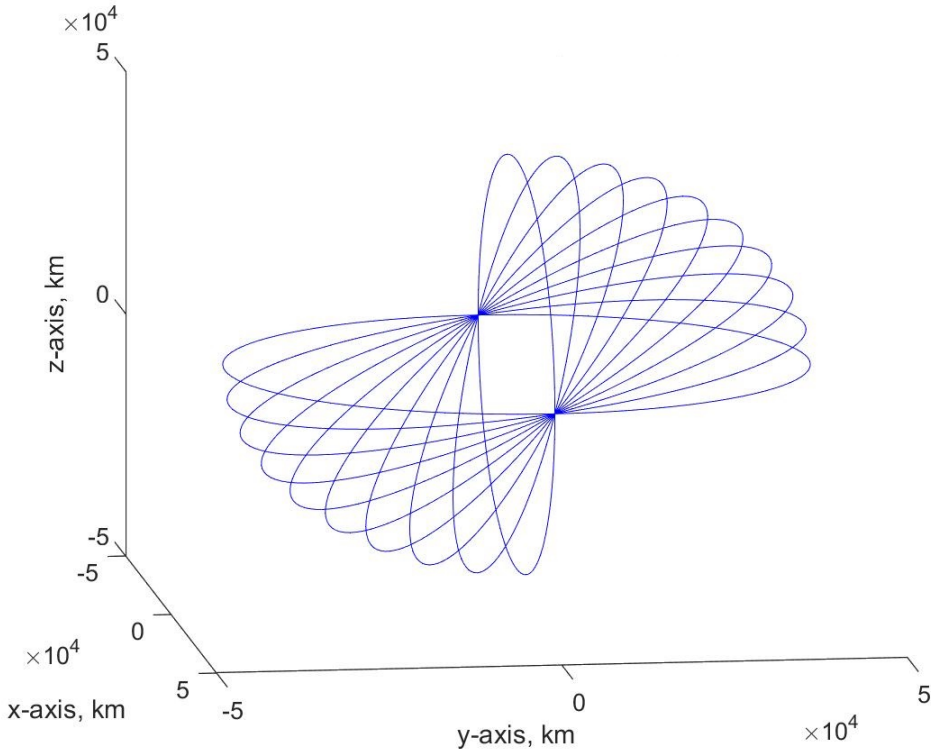

Figure 5.14. Orbits Tested for Non-coplanar, C2C, from GEO, Example

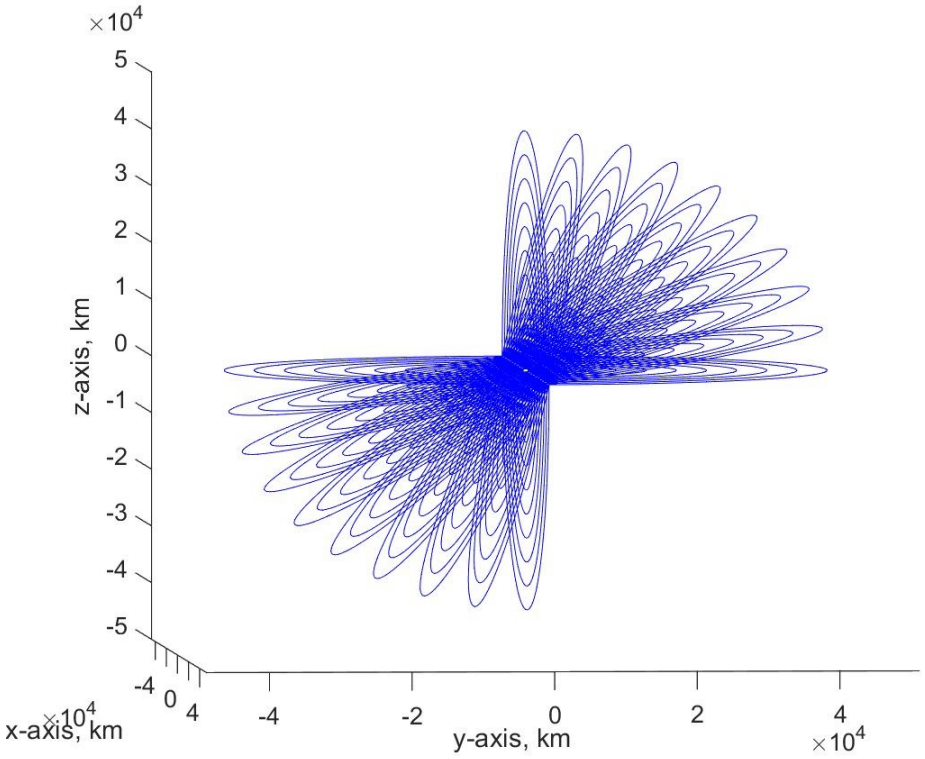

Figure 5.15. Orbits Tested for Non-coplanar, C2C, from GEO, Full Set

Table 5.13. Non-coplanar, C2C, from GEO Results, Example

Chief Inclination, °	Primer Vector km/s a_c/a_d=0.1	Minimize Δv^2 km/s a_c/a_d=0.1	% Variation , %
10	5.183565	5.200229	0.32
20	5.277196	5.315068	0.72
30	5.422030	5.466119	0.81
40	5.605218	5.652251	0.84
50	5.813966	5.8659593	0.89
60	6.037114	6.095810	0.97
70	6.265521	6.331825	1.1
80	6.491878	6.565472	1.1
90	6.710356	6.789565	1.2

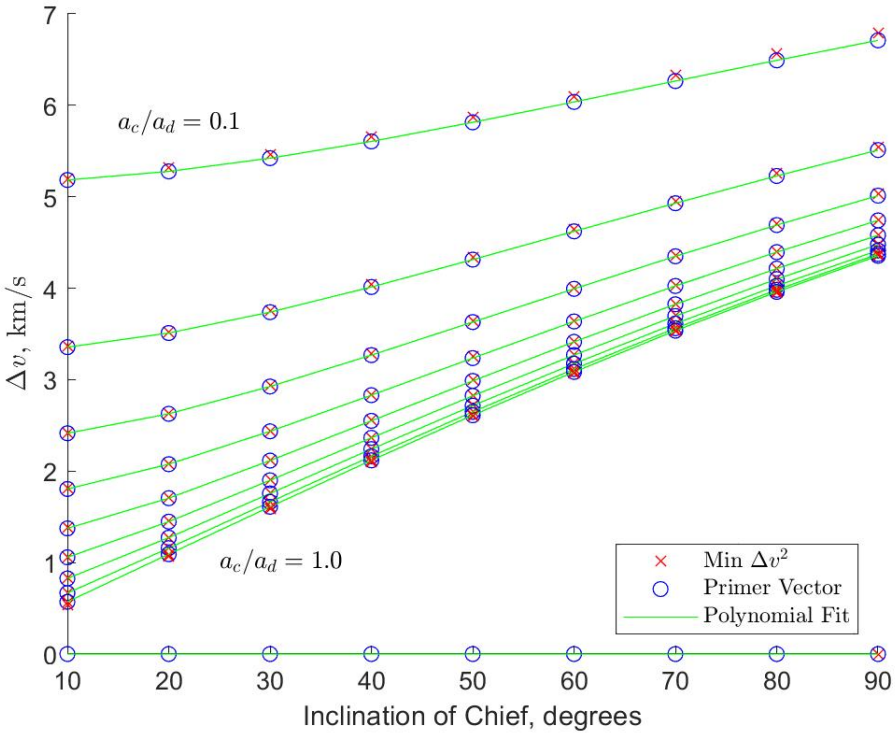

Figure 5.16. Non-coplanar, C2C, from GEO Results

5.2.2 C2E

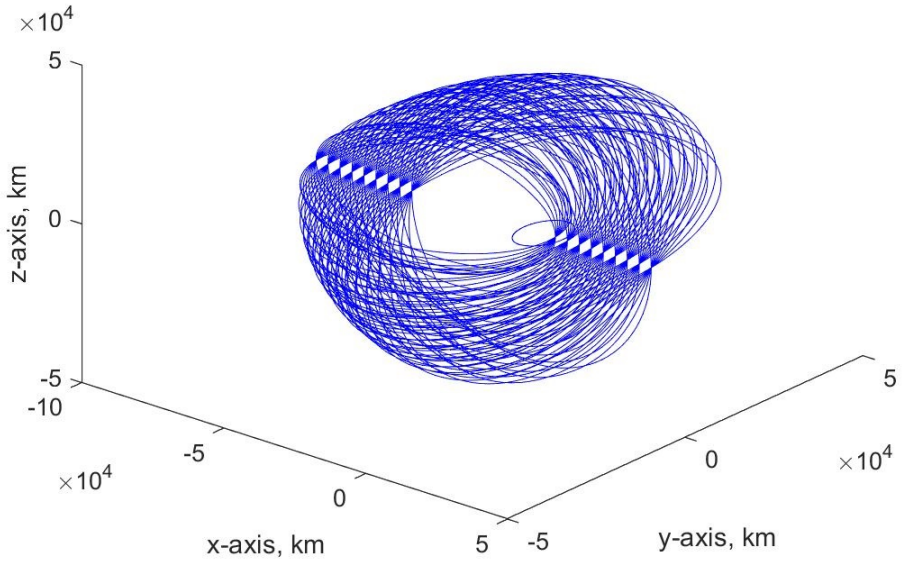

Figure 5.17. Orbits Tested for Non-coplanar, C2E, LEO to GEO

Table 5.14. Non-coplanar, C2E, LEO to GEO Results, Example

Chief Inclination, °	Primer Vector, km/s $e_c = 0.1$	Minimize Δv^2, km/s $e_c = 0.1$	% Variation , %
10	3.768920	3.771853	0.078
20	3.892255	3.907396	0.39
30	4.076897	4.091157	0.35
40	4.302183	4.317971	0.37
50	4.550599	4.571354	0.46
60	4.809042	4.837926	0.60
70	5.067972	5.106851	0.77
80	5.320409	5.369164	0.92
90	5.561010	5.617342	1.0

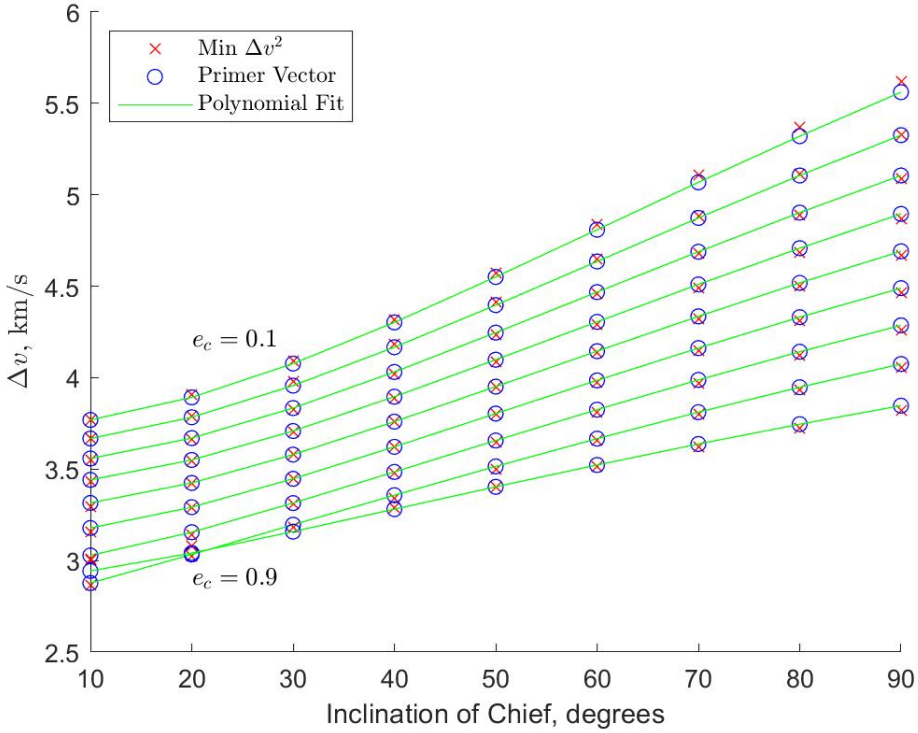

Figure 5.18. Non-coplanar, C2E, LEO to GEO Results

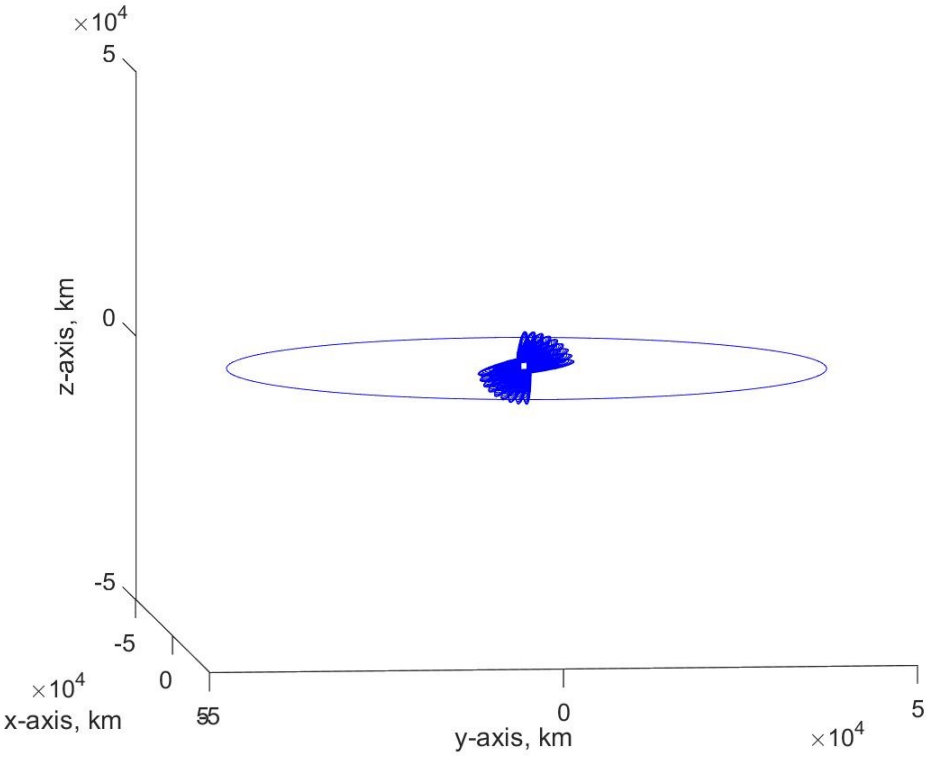

Figure 5.19. Orbits Tested for Non-coplanar, C2E, GEO to LEO

Table 5.15. Non-coplanar, C2E, GEO to LEO Results, Example

Chief Inclination, °	Primer Vector, km/s $e_c = 0.1$	Minimize Δv^2, km/s $e_c = 0.1$	% Variation , %
10	3.743645	3.776022	0.86
20	3.868283	3.926690	1.5
30	4.056336	4.126856	1.7
40	4.287733	4.378148	2.1
50	4.544820	4.651230	2.3
60	4.813880	4.927326	2.4
70	5.084695	5.206801	2.4
80	5.349602	5.480209	2.4
90	5.602723	5.739733	2.4

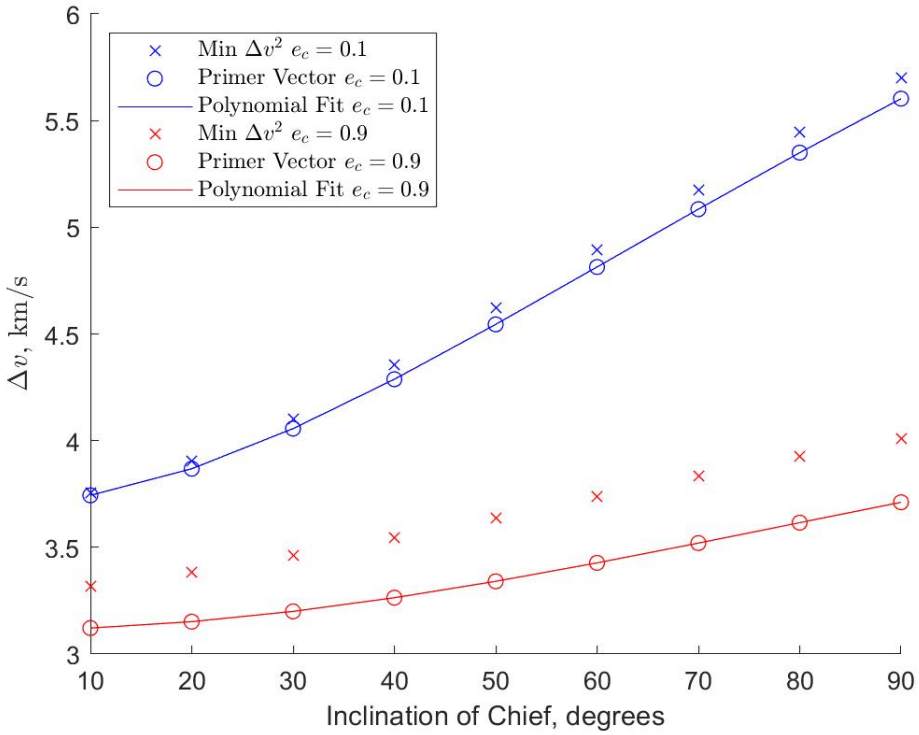

Figure 5.20. Non-coplanar, C2E, GEO to LEO Results, Selected

5.2.3 E2C

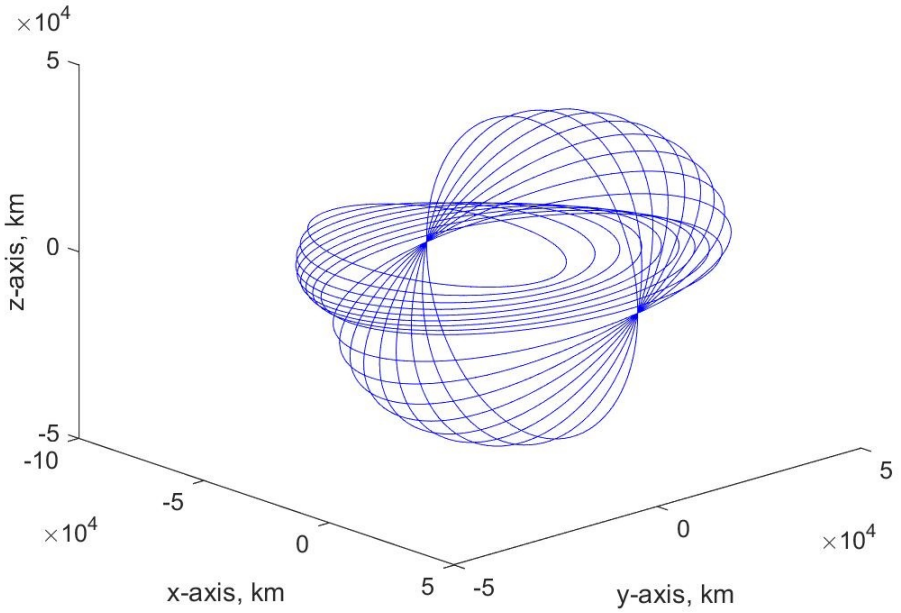

Figure 5.21. Orbits Tested for Non-coplanar, E2C, GEO to GEO

Table 5.16. Non-coplanar, E2C, GEO to GEO Results, Example

Chief Inclination, °	Primer Vector, km/s $e_d = 0.1$	Minimize Δv^2, km/s $e_d = 0.1$	% Variation , %
10	0.5312939	0.5273180	0.75
20	1.015662	1.010082	0.55
30	1.497067	1.490631	0.43
40	1.968754	1.960191	0.43
50	2.426458	2.416737	0.40
60	2.866381	2.854780	0.40
70	3.284992	3.272068	0.39
80	3.678983	3.664727	0.39
90	4.045276	4.029716	0.38

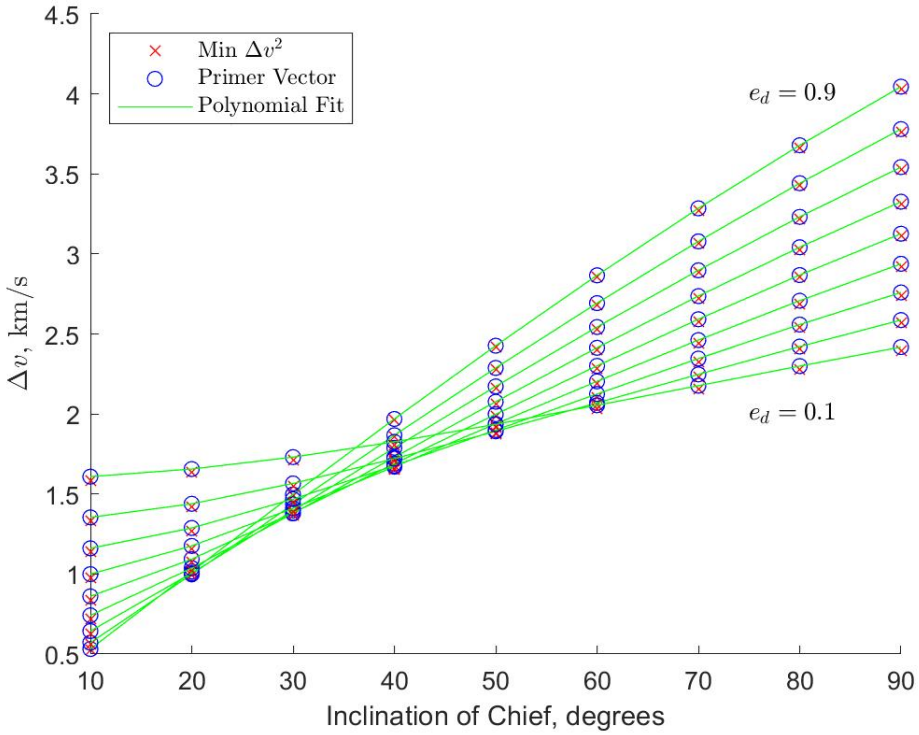

Figure 5.22. Non-coplanar, E2C, GEO to GEO Results

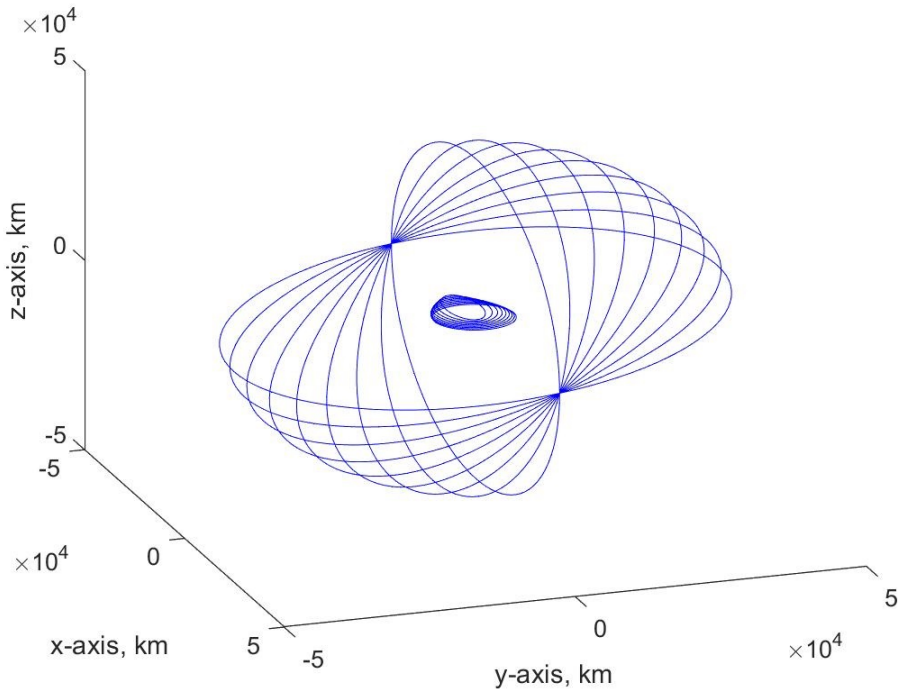

Figure 5.23. Orbits Tested for Non-coplanar, E2C, LEO to GEO

Table 5.17. Non-coplanar, E2C, LEO to GEO Results, Example

Chief Inclination, °	Primer Vector, km/s $e_d = 0.1$	Minimize Δv^2, km/s $e_d = 0.1$	% Variation , %
10	3.743645	3.730605	0.35
20	3.868281	3.860424	0.20
30	4.056337	4.059141	0.069
40	4.287732	4.296041	0.19
50	4.544819	4.548423	0.079
60	4.813881	4.811102	0.058
70	5.084693	5.074639	0.20
80	5.349600	5.331991	0.33
90	5.602731	5.577718	0.45

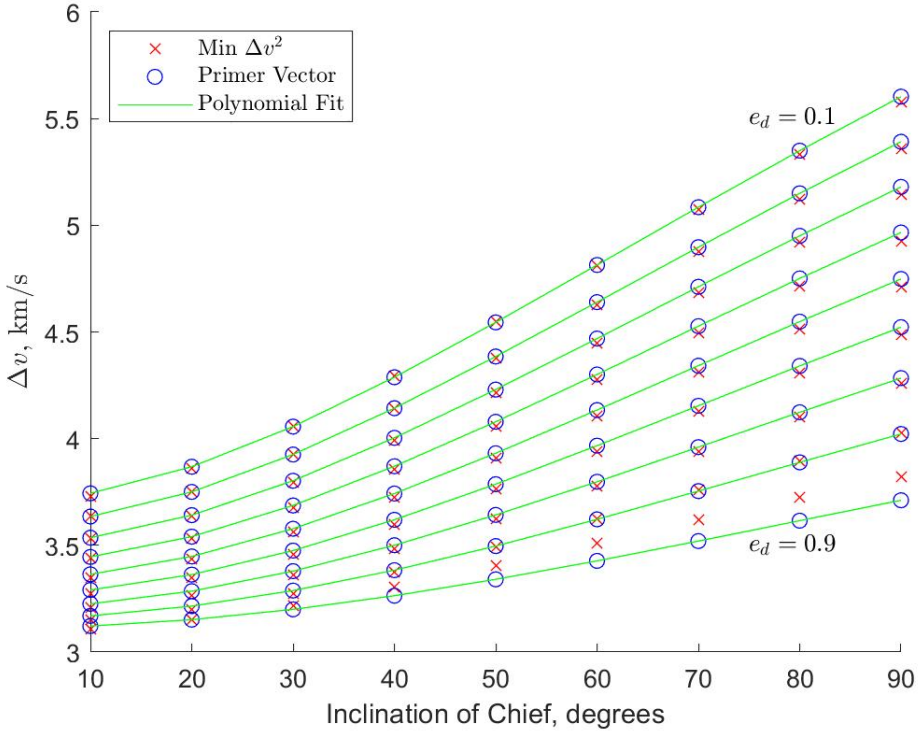

Figure 5.24. Non-coplanar, E2C, LEO to GEO Results

5.2.4

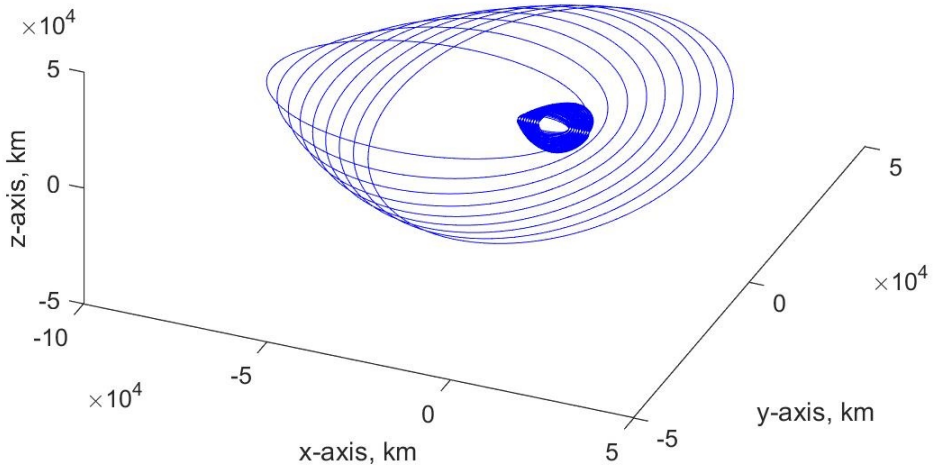

Figure 5.25. Orbits Tested for Non-coplanar, E2E, GEO to LEO

Table 5.18. Non-coplanar, E2E, GEO to LEO Results, Example

Chief Inclination, °	Primer Vector, km/s $e_c, e_d = 0.1$	Minimize Δv^2, km/s $e_c e_d = 0.1$	% Variation , %
10	3.642294	3.628646	0.37
20	3.757706	3.743205	0.39
30	3.931292	3.916576	0.37
40	4.144190	4.131243	0.31
50	4.380060	4.371491	0.20
60	4.626383	4.624459	0.042
70	4.873901	4.869412	0.092
80	5.115715	5.108184	0.15
90	5.346559	5.336495	0.19

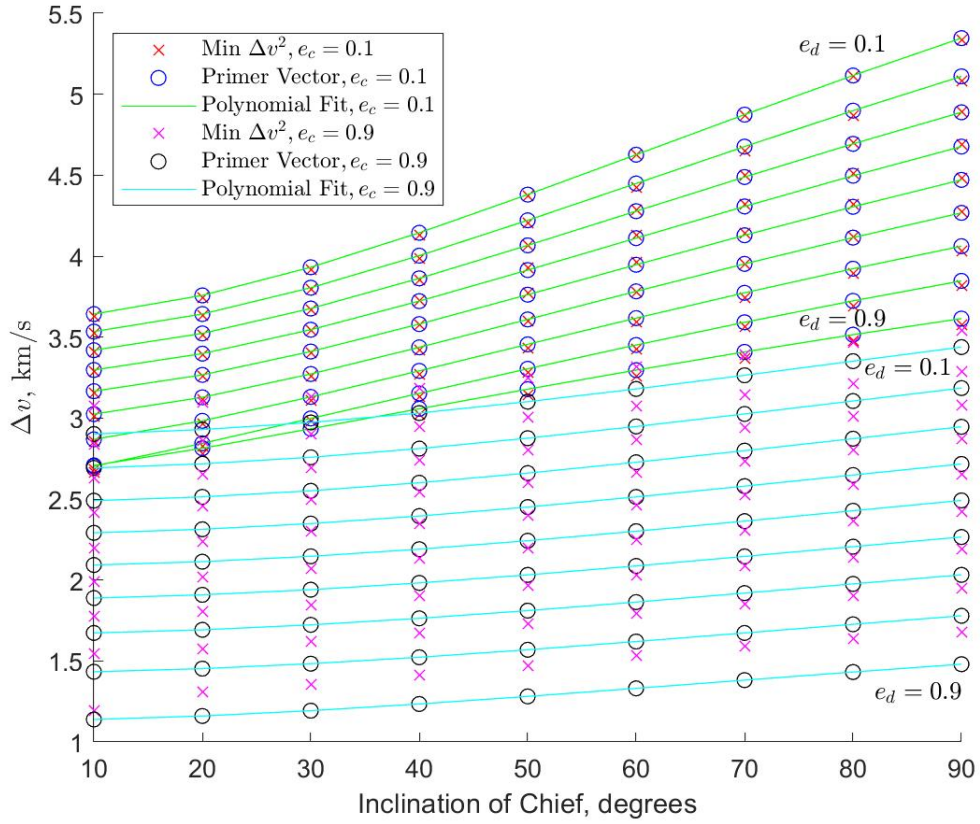

Figure 5.26. Non-coplanar, E2E, GEO to LEO Results

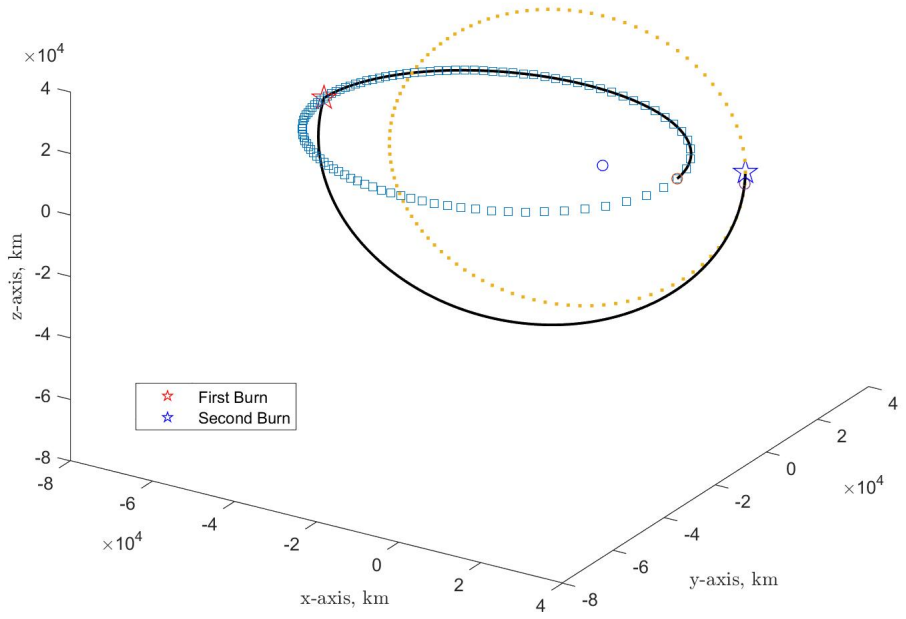

Figure 5.27. Non-coplanar, E2E, GEO to GEO Example Flight Path

Starting with coplanar results, C2C the primer vector method the most accurate, minimizing Δv^2 the fastest, and both an improvement over Lambert's problem. The larger the change in a_c compared to a_d, the larger the required Δv, linearly at first, then asymptotically as it approached a 0 ratio. In this case, the magnitude of the time improvement is not evident yet, since the code can take advantage of the symmetry of circles to vary only one true anomaly instead of both.

This became evident first in the C2E, GEO toLEO case when varying both true anomalies became required to achieve less than 13% variation between the Lambert solution results and primer vector results. The problem with the Lambert solution was that you needed to increase the accuracy of results by decreasing the intervals between true anomalies tested. After proven to become prohibitively time consuming to match the results, Lambert's

algorithm was dropped in order to focus on comparison between the remaining algorithms and potential trends in orbit types. This case revealed varying e_c could either increase or decrease Δv required based on change of a. The closer a_c was to a_d the the more direct, or less inverse the relationship became, depending on which ratio the change occurred. This case also first revealed the impact of singular matrices and a weakness in the minimum Δv^2 code that increases variation with higher eccentricities.

In E2C, it became evident that costs were equal in reverse maneuvers, meaning half of the results so far did not have to be included and the plan for future testing was cut in half.

In E2E, further weaknesses in the minimize Δv^2 code were realized with singularities apparent with eccentricity differences containing 1 significant figure. Most of these were remedied by adding 0.000001 onto one of them. Δv decreased with increasing e_c or e_d.

Moving on to non-coplanar, C2C showed an apparent direct linear relationship between change in i and Δv. % variation also increased overall, with higher %s at higher changes of i.

In C2E, higher e_c consistently became a shift to lower Δv, contrary to the shift that occurred due to varying a in the coplanar cases. With a large change in a, % variation became an issue for higher e changes.

In E2C, GEO to GEO there was an immediate flip in the coplanar realized relationship of higher e_d meaning higher Δv to the opposite. However, it reverts again since higher e_d also showed faster increases in Δv. In LEO to GEO, however, this flip was not evident, and the higher e_d did not indicate faster increases, but slower.

E2E revealed increasing e_c or e_d decreased Δv required, showing this combination can overwhelm the dominance previously observed in changing i.

The optimal flight path followed a perigee to apogee or apogee to perigee for all coplanar results. It wasn't until inclination changes that there were slight variations in this trend. If severely limited in computational power, starting a search in these areas of fastest and slowest speeds would be prudent.

THIS PAGE INTENTIONALLY LEFT BLANK

CHAPTER 6:
Conclusion and Future Work

6.1 Conclusion

Using MATLAB-based codes, this thesis compared algorithms for finding the optimal two-impulse transfer between orbits. Many cases of varying parameters were simulated to evaluate the algorithms for design of multi-client OOS missions, along with possible decision points for decision-makers based on client orbit types and differences.

The primer vector method was the most accurate and at least 150x faster than the Lambert method, but minimizing Δv^2 provided a 75-85% reduction in computation time within 2.4% compared to the primer vector method. Either method would be a great choice for implementation into a TSP over the Lambert method, depending on computational power pricing.

The primer vector method with the highest accuracy across all cases would be the best choice for clients occupying highly varied inclinations and eccentricities, especially when computational power represents a relatively small portion of the mission's budget. This would also be the preferred method without a complete understanding of client differences.

The minimizing Δv^2 method would be the best choice with many more clients in similar orbits. Examples could be servicing every SES satellite in GEO, or collecting a series of Starlink satellites for deorbiting.

6.2 Future Work

This thesis compared four algorithms for a single bi-impulsive orbit rendezvous solution. Two were seriously considered for updating the current state of successive node planning. There are other algorithms that have been developed that require coding and testing. The ones tested here, or others that prove better, must be implemented on a total cost plan for reaching increasing numbers of clients. The total cost plan should be considered dynamic and incorporate time between transfers and earned value into the cost function. This would

answer the question which clients to visit to earn the most and allow for adding clients mid-mission as opportunities arise. In addition to the cost function, there should be additional testing for the algorithms presented here to vary Ω and ω from COE, as well as relative position vector and velocity vector comparison. This could provide additional insight into the benefit of the primer method over the minimum Δv^2 or vice versa. After one of these algorithms is implemented into a TSP cost collection, TSP algorithms could be used to further reduce computational power, such as branch-and-bound, branch-and-cut, heuristic, or metaheuristic methods [23].

List of References

[1] Union of Concerned Scientists, "UCS satellite database," Jan. 1, 2022 [Online]. Available: https://www.ucsusa.org/resources/satellite-database

[2] SpaceX, "Capabilities & services," Mar. 5, 2022 [Online]. Available: https://www.spacex.com/media/Capabilities&Services.pdf

[3] Defense Innovation Unit, "Annual report FY2021," Annual Report, Defense Innovation Unit, Mountain View, CA, USA, 2021 [Online]. Available: https://assets.ctfassets.net/3nanhbfkr0pc/5JPfbtxBv4HLjn8eQKiUW9/cab09a726c2ad2ed197bdd2df343f385/Digital_Version_-_Final_-_DIU_-_2021_Annual_Report.pdf

[4] M. Sheetz, "For the first time ever, a robotic spacecraft caught an old satellite and extended its life," Apr. 17, 2020 [Online]. Available: https://www.cnbc.com/2020/04/17/northrop-grumman-mev-1-spacecraft-services-intelsat-901-satellite.html

[5] DARPA, "Robotic servicing of geosynchronous saetellites," Nov. 15, 2022 [Online]. Available: https://www.darpa.mil/program/robotic-servicing-of-geosynchronous-satellites

[6] J. Olsen, S. Butow, E. Felt, T. Cooley, and J. Mozer, "State of the space industrial base 2021," Summary Report, Defense Innovation Unit, Mountain View, CA, USA, 2021 [Online]. Available: https://assets.ctfassets.net/3nanhbfkr0pc/43TeQTAmdYrym5DTDrhjd3/1218bd749befdde511ac2c900db3a43b/Space_Industrial_Base_Workshop_2021_Summary_Report_-_Final_15_Nov_2021.pdf

[7] R. Smith, "Look ma! no (human) hands!" Mar. 5, 2007 [Online]. Available: https://web.archive.org/web/20090827034330/http://science.nasa.gov/headlines/y2007/05mar_nohands.htm

[8] Orbital Debris Program Office, "Legend : 3D/OD evolutionary model," Jul. 7, 2022 [Online]. Available: https://orbitaldebris.jsc.nasa.gov/modeling/legend.html

[9] B. W. Barbee, S. Alfano, E. Pinon, K. Gold, and D. Gaylor, "Design of spacecraft missions to remove multiple orbital debris objects," in *Aerospace Conference, 2011*, 2011 [Online]. Available: https://ieeexplore.ieee.org/document/5747303

[10] J. Bourjolly, O. Gurtuna, and A. Lyngvi, "On-orbit servicing: a time-dependent, moving-target traveling salesman problem," *Internation Transactions in Operational Research*, vol. 13, no. 5, Aug. 2006 [Online]. doi: https://doi.org/10.1111/j.1475-3995.2006.00558.x.

[11] D. Madakat, J. Morio, and D. Vanderpooten, "Biojective planning of an active debris removal mission," *Acta Astronautica*, vol. 84, no. 18, Dec. 2012 [Online]. doi: https://doi.org/10.1016/j.actaastro.2012.10.038.

[12] M. Romano, "Space flight mechanics," unpublished.

[13] H. Curtis, *Orbital Mechanics for Engineering Students*, 1st ed. Burlington, MA, USA: Elsevier Butterworth-Heinemann, 2005.

[14] I. Newton, *The Principia : Mathematical principles of natural philosophy*. Berkeley: University of California Press, 1999.

[15] International Astronomical Union, "Astronomical constants," Mar. 5, 2020 [Online]. Available: https://asa.hmnao.com/static/files/2021/Astronomical_Constants_2021.pdf

[16] M. Avendano and D. Mortari, "A closed-form solution to the minimum δv_{tot}^2 lambert's problem," *Celest Mech Dyn Astr*, vol. 106, no. 25, pp. 25–37, Nov. 2009.

[17] D. Lawden, *Optimal Trajectories for Space Navigation*, 1st ed. London, EN, UK: Butterworths, 1963.

[18] D. Eagle, "Optimal impulse orbital transfer," MATLAB Central File Exchange, Natick, MA, USA, Tech. Rep. 39160, 2022 [Online]. Available: https://www.mathworks.com/matlabcentral/fileexchange/39160-optimal-impulsive-orbital-transfer

[19] R. P. Brent, *Algorithms for Minimization Without Derivatives*, 1st ed. Englewood Cliffs, NJ, USA: Prentice-Hall, 1973.

[20] J. Lagarias, J. Reeds, M. Wright, and P. Wright, "Convergence properties of the nelder–mead simplex method in low dimensions," *Society for Industrial and Applied Mathematics journal on optimization*, vol. 9, no. 1, July 2006 [Online]. doi: https://doi.org/10.1137/S1052623496303470.

[21] National Aeronautics and Space Administration, "How long would a trip to mars take?" Sep. 14, 2022 [Online]. Available: https://image.gsfc.nasa.gov/poetry/venus/q2811.html

[22] National Aeronautics and Space Administration, "Mars fact sheet," Dec. 23, 2021 [Online]. Available: https://nssdc.gsfc.nasa.gov/planetary/factsheet/marsfact.html

[23] P. Toth and D. Vigo, *The Vehicle Routing Problem*, 1st ed. Philadelphia, PA, USA: Society for Industrial and Applied Mathematics, 2002.

[24] Oak Ridge National Laboratory, “Direction of discovery,” Nov. 15, 2022 [Online]. Available: https://www.olcf.ornl.gov/frontier/

[25] J. Walton, “Nvidia announces RTX 4090 coming october 12, RTX 4080 later,” Sep. 23, 2022 [Online]. Available: https://www.tomshardware.com/news/nvidia-geforce-rtx-4090-rtx-4080-price-release-date-specs-revealed

THIS PAGE INTENTIONALLY LEFT BLANK

Initial Distribution List

1. Defense Technical Information Center
   Ft. Belvoir, Virginia

2. Dudley Knox Library
   Naval Postgraduate School
   Monterey, California